

**Techniques for Investigating Scattering  
from the Subbottom in Shallow Water**

Contract Number: N00014-95-C-6019

Competitively Awarded

Prepared by:

Paul J. Vidmar  
Science Applications International Corporation  
1710 Goodridge Drive  
McLean, VA 22101

Prepared under contract for:

Joseph Gettrust  
Naval Research Laboratory-Stennis  
Code 7432  
Stennis Space Center, MS 39529-5004

August 1998

Approved for public release; distribution unlimited

19981113 013

## TABLE OF CONTENTS

ABSTRACT .....	ii
I. INTRODUCTION .....	1
II. PRELIMINARY RESEARCH .....	2
III. T-MATRIX APPROACH TO SCATTERING .....	3
A. Acoustic scattering .....	4
B. Elastic wave scattering .....	9
C. Multiple Scattering .....	15
1. Two Scatterers .....	15
2. N Scatterers .....	19
D. Layered Scatterer .....	22
E. Inhomogeneous Scatterer .....	24
F. Scattering from highly non-spherical shapes .....	25
G. Buried scatterers .....	29
3. Preliminaries .....	29
4. Integral Equations for the Surface $\sigma_0$ .....	31
5. Surface Fields .....	32
T-matrix for the Buried Scatterer .....	36
H. Scattering in a Waveguide .....	39
7. Source and Scatterer in the Same Layer .....	40
8. Source and Scatterer in Different Layers .....	46
9. Normal Mode Formulation .....	48
I. Summary .....	48
IV. P S COUPLING DUE TO GRADIENTS .....	48
A. Theory for Homogeneous Media .....	49
B. Theory for Heterogeneous Media .....	50
1. Weakly Coupled Potentials .....	51
2. Exact Coupled Potentials .....	54
3. Displacement and Stress for Exact Coupled Potentials .....	56
4. Decoupling of Exact Potentials .....	56
5. Resonance Frequencies .....	56
C. Summary .....	60
V. RECOMMENDATIONS .....	61
A. T-Matrix .....	61
B. Gradient Driven Coupling .....	62
REFERENCES .....	63

## ABSTRACT

This report reviews work carried out to identify promising techniques for determining the major acoustic mechanisms governing scattering from the subbottom in shallow water. Two approaches were investigated: (1) the application of T-matrix scattering theory to scattering from geological features in the subbottom, and (2) the coupled differential equation theory of gradient driven coupling of shear and compressional waves. T-matrix theory is well developed and has most of the characteristics needed for application to modeling scattering from the subbottom. T-matrix theory is a full wave approach, has few fundamental restrictions, includes both compressional and shear waves, applies to multiple structured scatterers of quite general shape, and can be formulated for a waveguide geometry. The basic theory of gradient driven coupling has been developed, but still has some features that are not well understood. The theory predicts "resonance frequencies" at which coupling between shear and compressional waves may be greatly enhanced. The resonance frequencies can be fairly high ( $>1$  kHz) for gradients estimated for volume inhomogeneities in shallow water sediments. The effects of the resonance have not been studied nor has a stochastic theory of gradient driven coupling been developed. This report concludes with some recommendations for future research to extend these approaches and to apply them to understanding scattering from the subbottom.

## I. INTRODUCTION

Researchers face formidable challenges in determining the major acoustical processes affecting acoustic propagation in shallow water and in developing the databases and stochastic models needed to accurately predict the acoustic field. The challenges arise from the complexity of the acoustic environment (water column and subbottom). The environment is characterized by variability on scales that affect propagation from Very Low Frequencies (5 Hz) to ultrasonic frequencies (1 MHz) frequencies. Internal waves, fine structure of the water column, subbottom inhomogeneities and layers, bottom bathymetry and roughness have all been suggested as significant environmental parameters. The challenge is to understand the physics of these processes well enough to develop the simplified models and databases needed for adequately predicting the performance of Navy acoustic systems.

An essential component of the solution to this problem is an understanding of scattering from the seafloor and subbottom. Scattering produces the reverberation, frequency spread, time spread, and angle spread that affect naval acoustic systems. Yamamoto<sup>1</sup> has developed a stochastic theory of scattering from measured velocity and density inhomogeneities that produced estimates of backscatter strength that are consistent with measured backscatter in the 100 Hz to 10 kHz frequency range. Other work by Anderson<sup>2</sup> demonstrated that bottom backscatter at 6.5 kHz could be explained by scattering from density and velocity fluctuations measured in cores. The fluctuations in density and velocity in the subbottom in shallow water are important sources of acoustic scattering that need to be included in Navy models and databases.

To develop adequate models and databases for predicting these phenomena, an accurate representation of seafloor structure (bathymetry, bottom roughness, and subbottom structure) is needed on the scale of an acoustic wavelength. Recent work has made progress toward providing structure on this scale. Yamamoto<sup>3</sup> has developed the technology of borehole tomography and produced the first direct measurements of velocity inhomogeneities (as opposed to distinct layers) in the upper 50 m of the subbottom on scales ranging from less than 1 m to about 10 m. Goff and Jordan<sup>4</sup> have developed a stochastic bathymetry model that has the potential for extrapolating multibeam bathymetry data to millimeter scales. Other work by Orsi<sup>5</sup> uses x-ray tomography of cores to provide millimeter to centimeter scale measurements of density fluctuations.

This report describes research carried out by Science Applications International Corporation from 1995 to 1998 to develop the technology for understanding scattering from the seafloor and subbottom in shallow water at frequencies from



100 Hz to 10 kHz. The overall objective of this research was to develop stochastic acoustic and geological models for accurate numerical simulation of the effects of scattering from the seafloor. There were three technical goals. First, to develop a quantitative understanding of the role of subbottom inhomogeneities in producing reverberation and FAT (frequency, angle, and time) spreads in shallow water. Second, to develop stochastic models describing subbottom parameters producing scattering. Third, to develop acoustic models for predicting FAT spreads and reverberation from stochastic geological models. Due to a funding shortfall, the scope of our work was reduced and focused on the first goal.

We concentrated on two theoretical approaches that looked promising for application to scattering from subbottom inhomogeneities. The first was the T-matrix approach to scattering. We examined this technique and found that it has all the attributes necessary for application to scattering from objects buried in the subbottom. The second was the coupled potential approach for predicting gradient driven coupling between shear and compressional waves. This approach appears suitable for application of the Born approximation for predicting scattering from subbottom velocity and density fluctuations. Both of these approaches are reviewed below.

As a result of our work, we recommend that additional research be carried out to develop the numerical implementation of both of these approaches for the prediction of time and angle spreading of acoustic signals.

## II. PRELIMINARY RESEARCH

We began our research with some two preconceived notions. The first of these was that we were looking for approaches with the fewest theoretical limitations. Our goal was to develop an approach that could be used for sensitivity studies to identify the major mechanisms and parameters that would be needed for modeling the performance of naval systems. To carry out these studies we felt that accuracy was paramount in the research model so that as many physical mechanisms as possible were included. The sensitivity studies, not our model, should identify the important mechanisms and parameters. The second notion was that the large gradients associated with volume inhomogeneities might make gradient driven coupling of shear and compressional waves a significant process in shallow water. This idea was based on the recent reports that velocity fluctuations could have gradients an order of magnitude larger than those previously considered.

### III. T-MATRIX APPROACH TO SCATTERING

Our research began with a survey of recent publications in the Journal of the Acoustical Society of America to identify potential approaches to scattering. By far, we found that the majority of publications between 1976 and 1994 dealing with scattering were based on the T-matrix approach or some variant of it. We found publications dealing with scattering of acoustic waves, scattering of elastic waves, multiple scattering, scattering by various shaped objects, scattering from objects with internal resonances, and scattering from objects in a waveguide. While the T-matrix approach has been applied to scattering from objects buried in the seafloor, it has not yet been applied to scattering from sedimentary layering in the subbottom. It appeared from this survey that the T-matrix approach should be examined for its suitability for predicting scattering from subbottom inhomogeneities.

Waterman<sup>6</sup> originally developed the T-matrix approach for acoustic scattering problems. The approach uses the Helmholtz integral equations that relate the scattered field to the incident field and an integral of the total field on the surface of the scattering object. The incident and scattered fields are expanded in terms of a set of basis functions, such as spherical harmonics. The essence of the T-matrix approach is to use two surface integral equations, one for an observation point inside the scattering object and the other for a point outside the scattering object, to obtain a relationship between the expansion coefficients of incident and scattered fields. The matrix relating the coefficients is the transition matrix, the "T-matrix". The T-matrix depends only on the shape of the scattering object and the boundary conditions. The only mathematical limitations imposed by the theory are that the shape of the scatterer allow an inscribed and circumscribed sphere for defining the spherical wave functions used as a basis set for the incident and scattered field. Otherwise, the scattering surface can have almost any shape.

The T-matrix approach proved to be very general and has been applied to scattering of elastic and electromagnetic waves. In these cases, the mathematics is more complicated than that for acoustic scattering because one must deal with vector fields and tensor Green's functions. Ref. 7 is a comprehensive listing of publications, as of 1988, extending and applying the T-matrix approach and Ref. 8 is collection of early work on the T-matrix. A unified view of T-matrix theory for acoustic, elastic, and electromagnetic problems is given in Ref. 9 while a recent review article<sup>10</sup> concentrates on application to scattering from structured objects with resonances.

For the research reported here, we examined papers on the application of T-matrix theory to elastic scattering<sup>9,11-16</sup>, scattering from objects with attenuation<sup>17,18</sup>, multiple scattering<sup>19-23</sup>, scattering from structured objects<sup>18,24-26</sup>, scattering from non-spherical objects<sup>27-32</sup>, scattering from objects in a layered medium<sup>33,34</sup>, and scattering in a waveguide<sup>35-37</sup>. Our major focus was to understand the theory well enough to determine the feasibility of applying it to scattering from subbottom inhomogeneities. We did not identify any fundamental limitations that would exclude it from this application.

#### A. Acoustic scattering

We will follow the approach of Waterman<sup>6</sup> in briefly outlining the derivation of the fundamental T-matrix equations. Waterman examines the total acoustic field,  $\Psi$ , being made up of an incident field,  $\Psi^i$ , and a scattered field,  $\Psi^s$ . His starting point is the Green's theorem for scalar fields<sup>9</sup> relating the fields inside and outside a bounding surface to the sources of the field and the field on the surface. This is essentially Huygen's principle. The geometry is shown in Fig. 1. There are no

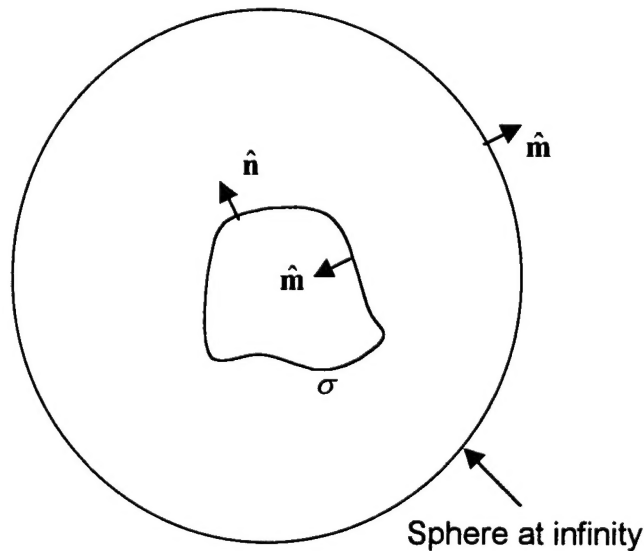


Figure 1. Geometry for a single scatterer.

sources within the scatterer. In this case the bounding surface is that of the scattering object ( $\sigma$ ) and a sphere at infinity. The volume we consider is all space excluding the interior of the scattering object, i. e., the interior of the scatterer is the exterior of our volume. On the surface ( $\sigma$ ) of the scatterer, the outward normal of the surface bounding our volume is  $\hat{\mathbf{m}}$  which is in the opposite direction to the outward normal of the surface bounding the scatterer,  $\hat{\mathbf{n}}$ . The

source is has a single frequency and has an  $\exp(-i\omega t)$  time dependence. There are two integral equations, one for an observation point in our volume and one for an observation point, outside our volume. For a point within the volume, Green's theorem is

$$\Psi(\mathbf{r}) = \Psi^i(\mathbf{r}) + \frac{1}{4\pi} \int d\sigma \hat{\mathbf{n}} \cdot \left[ \Psi_+(\mathbf{r}') \nabla g(k_p |\mathbf{r} - \mathbf{r}'|) - g(k_p |\mathbf{r} - \mathbf{r}'|) \nabla_+ \Psi(\mathbf{r}') \right] \quad (1)$$

where:  $\mathbf{r}$  is an observation point inside the volume,  $\mathbf{r}'$  is a point on the surface  $\sigma$ ,  $k_p = \omega/c_p$  is the wavenumber of the acoustic field,  $c_p$  is the sound speed of the medium,  $\Psi_+$  and  $\nabla_+ \Psi$  are the total field and its gradient on the surface of the scatterer (on the outside of the scatterer), and  $g$  is the free space scalar Green's function. The free space Green's function satisfies  $\nabla^2 g + k_p^2 g = 4\pi\delta(\mathbf{r} - \mathbf{r}')$  and is given by

$$g(k_p R) = ik_p h_0^{(1)}(k_p R) = \frac{e^{ik_p R}}{R}$$

where:  $R = |\mathbf{r} - \mathbf{r}'|$  and  $h_0^{(1)}$  is the Hankel function of the first kind of order zero. The Green's function represents an outgoing spherical wave from a source at  $\mathbf{r}'$ .

The second integral equation is

$$0 = \Psi^i(\mathbf{r}) + \frac{1}{4\pi} \int d\sigma \hat{\mathbf{n}} \cdot \left[ \Psi_+(\mathbf{r}') \nabla g(k_p |\mathbf{r} - \mathbf{r}'|) - g(k_p |\mathbf{r} - \mathbf{r}'|) \nabla_+ \Psi(\mathbf{r}') \right] \quad (2)$$

where the observation point  $\mathbf{r}$  is now outside the volume (inside the scatterer). This equation states that the incident field and the field generated by the virtual sources on the surface cancel inside the volume. It does not say that the total field inside the volume is zero. The field in the interior is given by the solution to the wave equation for the interior with boundary conditions and total field specified on the surface of the scatterer.

The next step is to expand the Green's function, the incident field, and the scattered field in terms of basis sets whose coefficients can be related through the boundary conditions on the surface of the scatterer. Waterman chose the partial wave solutions of the scalar Helmholtz equation,  $\nabla^2 \Psi + k_p^2 \Psi = 0$ , in spherical coordinates. (He also considered cylindrical coordinates.) In this case, the basis set is given by

$$\psi_{p,m,n}(k_p \mathbf{r}) = (\gamma_{m,n})^{1/2} h_n^{(1)}(k_p r) Y_{m,n}^p(\theta, \phi)$$

where:  $h_n^{(1)}$  are spherical Hankel functions of the first kind of order  $n$ ,  $Y_{m,n}^p$  are spherical harmonics,  $p$  is an index with two values (even or odd) indicating the parity of the spherical harmonic, and  $\gamma_{m,n}$  is a constant given by

$$\gamma_{m,n} = \begin{cases} (2n+1) & \text{for } m = 0 \\ 2(2n+1)(n-m)!/(n+m)! & \text{for } m \neq 0 \end{cases}$$

The spherical harmonics are given by

$$Y_{m,n}^p(\theta, \phi) = \begin{cases} \cos(m\phi) P_n^m(\cos\theta) & \text{for } p = \text{even} \\ \sin(m\phi) P_n^m(\cos\theta) & \text{for } p = \text{odd} \end{cases}$$

where  $P_n^m$  are the associated Legendre polynomials. We choose a coordinate system with an origin inside the scattering object. Since there are no sources within the scattering object, we expand the incident field in terms of regular wave functions ( $\text{Re}\psi_{p,m,n}$ ), i. e. wave functions that do not have singularities at the origin. For spherical coordinates the regular wave functions are

$$\text{Re}\psi_{p,m,n}(k_p \mathbf{r}) = \gamma_{m,n}^{1/2} j_n(k_p r) Y_{m,n}^p(\theta, \phi)$$

The incident field is then

$$\Psi^i = \sum a_n \text{Re}\psi_n$$

in which we have collapsed the multiple indices ( $p, m, n$ ) to a single index,  $n$ . Expansions for plane waves and point sources in homogeneous media are available for spherical and cylindrical coordinate systems.

The Green's function for free space may be expanded in terms of the eigenfunctions as<sup>38</sup>

$$g(k_p | \mathbf{r} - \mathbf{r}') = ik_p \sum \psi_n(k_p \mathbf{r}_>) \text{Re} \psi_n(k_p \mathbf{r}_<)$$

where:  $\mathbf{r}_<$  and  $\mathbf{r}_>$  refer to the lesser and greater of  $\mathbf{r}$  and  $\mathbf{r}'$ . If we consider the region outside a sphere enclosing the scattering object, express the scattered field as the expansion

$$\Psi^s = \sum f_n \psi_n$$

use the eigenfunction expansion for the Green's function, and note that  $r' > r$ , then Eq. (1) becomes

$$f_n = \frac{ik_p}{4\pi} \int d\sigma \hat{\mathbf{n}} \cdot \left[ \Psi_+(\mathbf{r}') \nabla \text{Re} \psi_n(k_p \mathbf{r}') - \text{Re} \psi_n(k_p \mathbf{r}') \nabla_+ \Psi(\mathbf{r}') \right] \quad (3)$$

Similarly, for a region inside a sphere contained within the scattering object, Eq. (2) becomes

$$a_n = -\frac{ik_p}{4\pi} \int d\sigma \hat{\mathbf{n}} \cdot \left[ \Psi_+(\mathbf{r}') \nabla \psi_n(k_p \mathbf{r}') - \psi_n(k_p \mathbf{r}') \nabla_+ \Psi(\mathbf{r}') \right] \quad (4)$$

To proceed further, we need to consider the boundary conditions on the scattering object. The boundary conditions relate the total field to its gradient on the surface of the object. We will consider two boundary conditions: the Neumann boundary condition ( $\hat{\mathbf{n}} \cdot \nabla_+ \Psi = 0$ ), and a penetrable boundary condition having continuous pressure and normal component of velocity. Expanding the total field in a complete set of functions allows us to solve Eqs 3 and 4 can then for  $a_n$  and  $f_n$ . The matrix relating them is the T-matrix.

For the Neumann boundary condition, we choose to expand the field on the surface of the object in terms of the regular eigenfunctions, which we assume forms a complete set on the surface of the object, as

$$\Psi_+ = \sum \alpha_n \text{Re} \psi_n$$

Substituting into Eqs. 3 and 4 yields the following two equations in matrix and vector notation.

$$\mathbf{a} = i\mathbf{Q}^T \alpha \quad (5)$$

$$\mathbf{f} = i\text{Re}(\mathbf{Q}^T) \alpha \quad (6)$$

The matrix  $\mathbf{Q}$  is given by

$$Q_{m,n} = \frac{k_p}{4\pi} \int d\sigma \hat{\mathbf{n}} \cdot \nabla (\psi_m(k_p \mathbf{r}')) \text{Re} \psi_n(k_p \mathbf{r}')$$

$$\text{Re} Q_{m,n} = \frac{k_p}{4\pi} \int d\sigma \hat{\mathbf{n}} \cdot \nabla (\text{Re} \psi_m(k_p \mathbf{r}')) \text{Re} \psi_n(k_p \mathbf{r}')$$

Eliminating  $\alpha$  from Eqs. 5 and 6 yields the T matrix

$$\mathbf{f} = \mathbf{T} \mathbf{a}$$

where

$$\mathbf{T} = -\text{Re}(\mathbf{Q}^T)(\mathbf{Q}^T)^{-1}$$

The next example is the usual acoustic boundary conditions on the surface of the scattering object—continuity of pressure and the normal component of the velocity. Primes will denote quantities in the interior of the object. The boundary conditions on the surface are

$$\hat{\mathbf{n}} \cdot \nabla_+ \Psi = \hat{\mathbf{n}} \cdot \nabla_- \Psi$$

$$\rho \Psi_+ = \rho \Psi_-$$

Assuming the interior to be homogeneous, the wavefunctions  $\{\text{Re} \Psi_n(k'_p \mathbf{r})\}$  form a complete set and the field in the interior can be expanded as

$$\Psi_- = \sum \beta_n \text{Re} \psi_n(k'_p \mathbf{r})$$

Using the boundary conditions to express  $\Psi_+$  in terms of  $\Psi_-$ , the eigenfunction expansion of  $\Psi_-$ , and eliminating the coefficient vector  $\beta$  results in the following expression for the  $Q$  matrix that defines the T-matrix.

$$Q_{m,n} = \frac{k_p}{4\pi} \int d\sigma \hat{n} \cdot \left\{ \frac{\rho'}{\rho} [\text{Re} \psi_m(k'_p \mathbf{r}') \nabla \psi_n(k_p \mathbf{r}') - \nabla [\text{Re} \psi_m(k'_p \mathbf{r}')] \psi_n(k_p \mathbf{r}')] \right\}$$

Attenuation can be included by making  $k'_p$  complex.

The final step is the evaluation of the infinite size T-matrix. This can be done by solving for the T matrix of rank  $n$  and then increasing  $n$  until the matrix elements converge. Reference 10 discusses more numerically efficient approaches.

The advantages of the T-matrix over other approaches to scattering can be seen from the examples above. The equations for  $Q$ , and hence the T-matrix depend only on the size and shape of the scatterer and not on the incident field. Once evaluated, the T-matrix can be used to find the scattered field produced by any incoming field. Another advantage is that the methodology is not restricted to objects of a certain shape. The integral involved is a surface integral. Once an integration algorithm is developed, it can be applied to any surface. Unlike the eigenfunction expansion method, the T-matrix is not restricted to objects of a particular shape having the symmetry of the coordinate system.

## B. Elastic wave scattering

The T-matrix for elastic wave scattering is much more complicated than that for acoustic scattering. The basic reason for this is that the basis functions become a set of vectors, rather than a single scalar, and the Green's function becomes a tensor quantity. For our discussion below we follow the presentation in Ref. 14.

We consider an infinite, homogeneous, isotropic medium of density  $\rho$  and Lamé parameters  $\lambda$  and  $\mu$ . The embedded scatterer has different properties  $\rho_1$ ,  $\lambda_1$ , and  $\mu_1$ . The only condition on the surface of the scatterer is that it be smooth, having a normal vector that changes continuously over the surface. The geometry is still that of Fig. 1. The incident wave is time harmonic with frequency  $\omega$  and time dependence  $e^{(-i\omega t)}$ . The vector displacement field  $\mathbf{u}(\mathbf{r})$  is made up of the incident displacement  $\mathbf{u}^i(\mathbf{r})$  and the scattered displacement  $\mathbf{u}^s(\mathbf{r})$  where  $\mathbf{r}$  is the position vector of an observation point. The equation of motion is

$$\nabla \cdot \tilde{\mathbf{T}} + \rho \omega^2 \mathbf{u} = 0 \quad (7)$$



where  $\tilde{\mathbf{T}}$  is the stress tensor, which is defined in terms of the displacement as

$$\tilde{\mathbf{T}} = \lambda \tilde{\mathbf{I}} \nabla \cdot \mathbf{u} + \mu (\nabla \mathbf{u} + \mathbf{u} \nabla)$$

$\tilde{\mathbf{I}}$  is the identity tensor. The traction  $\mathbf{t}$  is given by  $\mathbf{t} = \hat{\mathbf{n}} \cdot \tilde{\mathbf{T}}$ .

The first step in the derivation of the T-matrix for elastic wave scattering is to obtain integral equations similar to Eqs. 1 and 2. These integral equations relate the incident and scattered field to the integral over the surface of the scatterer. We begin by defining the Green's tensor  $\tilde{\mathbf{G}}$  and a Green's stress tensor  $\tilde{\mathbf{S}}$  as being related to a point source at  $\mathbf{r}'$ . The Green's tensor is the solution to

$$\nabla \cdot \tilde{\mathbf{S}} + \rho \omega^2 \tilde{\mathbf{G}} = -\tilde{\mathbf{I}} \delta(\mathbf{r} - \mathbf{r}') \quad (8)$$

where  $\tilde{\mathbf{S}}$  is the stress tensor (rank 3) defined in terms of the Green's tensor

$$\tilde{\mathbf{S}} = \lambda \tilde{\mathbf{I}} \nabla \cdot \tilde{\mathbf{G}} + \mu (\nabla \tilde{\mathbf{G}} + \tilde{\mathbf{G}} \nabla)$$

In indicial notation, the last term in the definition of  $\tilde{\mathbf{S}}$  is defined as  $\partial_i G_{jk} + \partial_j G_{ik}$  where  $\partial_i = \partial/\partial x_i$  and  $i, j$ , and  $k$  refer to the components of the position vector. The solution of these two equations is the Green's tensor given by<sup>9,39</sup>

$$G_{ij} = \frac{1}{4\pi\rho\omega^2} \left\{ \delta_{ij} k_s^2 g(k_s |\mathbf{r} - \mathbf{r}'|) - \partial_i \partial_j [g(k_p |\mathbf{r} - \mathbf{r}'|) - g(k_s |\mathbf{r} - \mathbf{r}'|)] \right\}$$

Where:  $g$  is the scalar Green's function defined above,  $k_p^2 = \rho\omega^2/(\lambda + 2\mu)$  is the square of the compressional wavenumber, and  $k_s^2 = \rho\omega^2/\mu$  is the square of the shear wavenumber.

The integral equation relating the displacement field to the field on the surface of the scatterer is obtained from Eqs. 7 and 8. We apply the divergence theorem to Eq. 7 postmultiplied by  $\tilde{\mathbf{G}}$  and Eq. 8 premultiplied by  $\mathbf{u}$  to obtain

$$\mathbf{u}(\mathbf{r}) = \mathbf{u}^i(\mathbf{r}) + \int d\sigma \left\{ \mathbf{u} \cdot \hat{\mathbf{n}} \cdot \tilde{\mathbf{S}} - \hat{\mathbf{n}} \cdot \tilde{\mathbf{T}} \cdot \tilde{\mathbf{G}} \right\} \quad \text{for } \mathbf{r} \text{ outside } \sigma \quad (9)$$

$$0 = \mathbf{u}^i(\mathbf{r}) + \int d\sigma \left\{ \mathbf{u} \cdot \hat{\mathbf{n}} \cdot \tilde{\mathbf{S}} - \hat{\mathbf{n}} \cdot \tilde{\mathbf{T}} \cdot \tilde{\mathbf{G}} \right\} \quad \text{for } \mathbf{r} \text{ inside } \sigma \quad (10)$$

We note that the quantities inside the integrals depend on both  $\mathbf{r}$  and  $\mathbf{r}'$  where  $\mathbf{r}'$  is a point on the surface and that  $d\sigma$  is the area element at  $\mathbf{r}'$ .

The next step in obtaining the T-matrix is to define the basis functions we will use to expand the field quantities. In three dimensions the displacement vector can be written as the sum of three vectors derived from scalar potentials as

$$\mathbf{u}(\mathbf{r}) = \nabla P + k_s \nabla \times (\mathbf{r}Q) + \nabla \times \nabla \times (\mathbf{r}S)$$

where: compressional waves are described by the potential  $P$  and shear waves by the potentials  $Q$  and  $S$ . In analogy to this equation there are three sets of basis functions

$$\vec{\phi}_{pnm}(\mathbf{r}) = \begin{cases} (k_p/k_s)^{1/2} \zeta_n \nabla [h_n(k_p \mathbf{r}) P_n^m(\cos \theta) \cos m\varphi] & p = \text{even} \\ (k_p/k_s)^{1/2} \zeta_n \nabla [h_n(k_p \mathbf{r}) P_n^m(\cos \theta) \cos m\varphi] & p = \text{odd} \end{cases}$$

$$\vec{\psi}_{pnm}(\mathbf{r}) = \begin{cases} k_s \eta_n \nabla \times [\mathbf{r} h_n(k_s \mathbf{r}) P_n^m(\cos \theta) \cos m\varphi] & p = \text{even} \\ k_s \eta_n \nabla \times [\mathbf{r} h_n(k_s \mathbf{r}) P_n^m(\cos \theta) \cos m\varphi] & p = \text{odd} \end{cases}$$

$$\vec{\chi}_{pnm}(\mathbf{r}) = \frac{1}{k_s} \nabla \times \vec{\psi}_{pnm}(\mathbf{r})$$

Arrows over quantities in the above equations indicate that they are vectors. The constants  $\zeta_n$  and  $\eta_n$  are give by

$$\zeta_n = \left[ \varepsilon_n \frac{(2n+1)(n-m)!}{4\pi(n+m)!} \right]$$

$$\eta_n = \left[ \varepsilon_n \frac{(2n+1)(n-m)!}{4\pi n(n+1)(n+m)!} \right]$$

where  $\varepsilon_0 = 1$  and  $\varepsilon_n = 2$  ( $n > 0$ ) is the Neumann factor. Basis functions that are regular at the origin are obtained by replacing  $h_n$  with  $j_n$ .

The quantities appearing in Eqs. 9 and 10 can now be expanded in terms of the basis functions.

$$\mathbf{u}^i(\mathbf{r}) = \sum_{pnm} [A_{pnm} \text{Re} \bar{\phi}_{pnm}(\mathbf{r}) + B_{pnm} \text{Re} \bar{\psi}_{pnm}(\mathbf{r}) + C_{pnm} \text{Re} \bar{\chi}_{pnm}(\mathbf{r})]$$

$$\mathbf{u}^s(\mathbf{r}) = \sum_{pnm} [\alpha_{pnm} \text{Re} \bar{\phi}_{pnm}(\mathbf{r}) + \beta_{pnm} \text{Re} \bar{\psi}_{pnm}(\mathbf{r}) + \gamma_{pnm} \text{Re} \bar{\chi}_{pnm}(\mathbf{r})]$$

$$\bar{\mathbf{G}}(\mathbf{r}, \mathbf{r}') = \frac{i}{(\rho\omega)^2} \sum_{pnm} k_s [\bar{\phi}_{pnm}(\mathbf{r}_<) \text{Re} \bar{\phi}_{pnm}(\mathbf{r}_>) + \bar{\psi}_{pnm}(\mathbf{r}_<) \text{Re} \bar{\psi}_{pnm}(\mathbf{r}_>) + \bar{\chi}_{pnm}(\mathbf{r}_<) \text{Re} \bar{\chi}_{pnm}(\mathbf{r}_>)]$$

The equation for  $\bar{\mathbf{G}}(\mathbf{r}, \mathbf{r}')$  follows from the expansion of the scalar Green's functions in terms of the basis sets in the expression for  $G_{ij}$  given above.

The integral equation for points inside a sphere within the scattering volume (Eq. 9) becomes, noting that  $r < r'$ ,

$$\sum_{pnm} [A_{pnm} \text{Re} \bar{\phi}_{pnm}(\mathbf{r}) + B_{pnm} \text{Re} \bar{\psi}_{pnm}(\mathbf{r}) + C_{pnm} \text{Re} \bar{\chi}_{pnm}(\mathbf{r})] = \quad (11)$$

$$- \sum_{pnm} \int d\sigma \{ \mathbf{u}(\mathbf{r}') \cdot \hat{\mathbf{n}} \cdot \bar{\mathbf{S}}_{pnm}(\mathbf{r}, \mathbf{r}') - \hat{\mathbf{n}} \cdot \bar{\mathbf{T}}(\mathbf{r}') \cdot \bar{\mathbf{G}}_{pnm}(\mathbf{r}, \mathbf{r}') \}$$

where the subscripts on the Green's tensor and Green's stress tensor denote terms in their expansions for  $r < r'$  given below.

$$\bar{\mathbf{G}}(\mathbf{r}, \mathbf{r}') = \frac{i}{(\rho\omega)^2} \sum_{pnm} k_s [\bar{\phi}_{pnm}(\mathbf{r}') \text{Re} \bar{\phi}_{pnm}(\mathbf{r}) + \bar{\psi}_{pnm}(\mathbf{r}') \text{Re} \bar{\psi}_{pnm}(\mathbf{r}) + \bar{\chi}_{pnm}(\mathbf{r}') \text{Re} \bar{\chi}_{pnm}(\mathbf{r})]$$

$$\bar{\mathbf{S}}(\mathbf{r}, \mathbf{r}') = \frac{ik_s}{(\rho\omega)^2} \{ \lambda \bar{\mathbf{I}} \text{Re} \bar{\phi}_{pnm}(\mathbf{r}) \nabla' \cdot \bar{\phi}_{pnm}(\mathbf{r}') + \mu [\nabla' \bar{\phi}_{pnm}(\mathbf{r}') + \bar{\phi}_{pnm}(\mathbf{r}') \nabla'] \text{Re} \bar{\phi}_{pnm}(\mathbf{r}) \}$$

$$+ \frac{i\mu k_s}{(\rho\omega)^2} \{ [\nabla' \bar{\psi}_{pnm}(\mathbf{r}') + \bar{\psi}_{pnm}(\mathbf{r}') \nabla'] \text{Re} \bar{\psi}_{pnm}(\mathbf{r}) + \mu [\nabla' \bar{\chi}_{pnm}(\mathbf{r}') + \bar{\chi}_{pnm}(\mathbf{r}') \nabla'] \text{Re} \bar{\chi}_{pnm}(\mathbf{r}) \}$$

Applying the same procedure to Eq. 10, and recalling that  $r < r'$  for this case, yields the following equation for the expansion coefficients of the scattered field.

$$\sum_{pnm} [\alpha_{pnm} \vec{\phi}_{pnm}(\mathbf{r}) + \beta_{pnm} \vec{\psi}_{pnm}(\mathbf{r}) + \gamma_{pnm} \vec{\chi}_{pnm}(\mathbf{r})] = \quad (12)$$

$$- \sum_{pnm} \int d\sigma \{ \mathbf{u}(\mathbf{r}') \cdot \hat{\mathbf{n}} \cdot \vec{\mathbf{S}}_{pnm}(\mathbf{r}', \mathbf{r}) - \hat{\mathbf{n}} \cdot \vec{\mathbf{T}}(\mathbf{r}') \cdot \vec{\mathbf{G}}_{pnm}(\mathbf{r}', \mathbf{r}) \}$$

where  $\vec{\mathbf{G}}_{pnm}(\mathbf{r}', \mathbf{r})$  is obtained by interchanging  $\mathbf{r}$  and  $\mathbf{r}'$  in the above expression for  $\vec{\mathbf{G}}_{pnm}(\mathbf{r}, \mathbf{r}')$  and

$$\begin{aligned} \vec{\mathbf{S}}(\mathbf{r}', \mathbf{r}) = & \frac{ik_s}{(\rho\omega)^2} \{ \lambda \vec{\mathbf{I}} \nabla' \cdot \text{Re} \vec{\phi}_{pnm}(\mathbf{r}') \vec{\phi}_{pnm}(\mathbf{r}) + \mu [\nabla' \text{Re} \vec{\phi}_{pnm}(\mathbf{r}') + \text{Re} \vec{\phi}_{pnm}(\mathbf{r}') \nabla'] \vec{\phi}_{pnm}(\mathbf{r}) \\ & + \frac{i\mu k_s}{(\rho\omega)^2} \{ [\nabla' R \vec{\psi}_{pnm}(\mathbf{r}') + \text{Re} \vec{\psi}_{pnm}(\mathbf{r}') \nabla'] \vec{\psi}_{pnm}(\mathbf{r}) \\ & + \mu [\nabla' \text{Re} \vec{\chi}_{pnm}(\mathbf{r}') + \text{Re} \vec{\chi}_{pnm}(\mathbf{r}') \nabla'] \vec{\chi}_{pnm}(\mathbf{r}) \} \end{aligned}$$

Equations 11 and 12 do not reduce to the simple relationship between an expansion coefficient and a surface integral, as was the case for acoustic scattering (Eqs. 5 and 6). To obtain a similar result for elastic scattering, we multiply Eq. 11 successively by  $\text{Re} \vec{\phi}_{pnm}(\mathbf{r})$ ,  $\text{Re} \vec{\psi}_{pnm}(\mathbf{r})$ , and  $\text{Re} \vec{\chi}_{pnm}(\mathbf{r})$ , integrate over all angles, use the orthogonality relations of spherical harmonics, and perform a little algebra to obtain

$$\begin{aligned} A_{pnm} = & -\frac{ik_s}{(\rho\omega)^2} \int d\sigma \{ \mathbf{u}(\mathbf{r}') \cdot \hat{\mathbf{n}} \cdot [\lambda \vec{\mathbf{I}} \nabla' \cdot \vec{\phi}_{pnm}(\mathbf{r}') + \mu \nabla' \vec{\phi}_{pnm}(\mathbf{r}') + \mu \vec{\phi}_{pnm}(\mathbf{r}') \nabla'] \\ & - \hat{\mathbf{n}} \cdot \vec{\mathbf{T}}(\mathbf{r}') \cdot \vec{\phi}_{pnm}(\mathbf{r}') \} \\ B_{pnm} = & -\frac{ik_s}{(\rho\omega)^2} \int d\sigma \{ \mathbf{u}(\mathbf{r}') \cdot \hat{\mathbf{n}} \cdot [\mu \nabla' \vec{\psi}_{pnm}(\mathbf{r}') + \mu \vec{\psi}_{pnm}(\mathbf{r}') \nabla'] - \hat{\mathbf{n}} \cdot \vec{\mathbf{T}}(\mathbf{r}') \cdot \vec{\psi}_{pnm}(\mathbf{r}') \} \\ C_{pnm} = & -\frac{ik_s}{(\rho\omega)^2} \int d\sigma \{ \mathbf{u}(\mathbf{r}') \cdot \hat{\mathbf{n}} \cdot [\mu \nabla' \vec{\chi}_{pnm}(\mathbf{r}') + \mu \vec{\chi}_{pnm}(\mathbf{r}') \nabla'] - \hat{\mathbf{n}} \cdot \vec{\mathbf{T}}(\mathbf{r}') \cdot \vec{\chi}_{pnm}(\mathbf{r}') \} \end{aligned}$$

Equation 12 yields similar expressions, with the basis functions replaced by regular basis functions, for the coefficients of the scattered field.

As was the case for acoustic scattering, we need to employ the boundary conditions on the scatterer to proceed further. As an example, we consider a cavity with stress vanishing on the surface of the scatterer. The boundary condition is  $\hat{\mathbf{n}} \cdot \tilde{\mathbf{T}}(\mathbf{r}') = 0$  for  $\mathbf{r}'$  on  $\sigma$ . We expand the surface displacement in terms of the regular basis set as

$$\mathbf{u}(\mathbf{r}') = \sum_{qij} [a_{qij} \text{Re} \tilde{\phi}_{qij}(\mathbf{r}') + b_{qij} \text{Re} \tilde{\psi}_{qij}(\mathbf{r}') + c_{qij} \text{Re} \tilde{\chi}_{qij}(\mathbf{r}')] ]$$

in which we have used different subscripts to identify the basis functions and coefficients. After substituting this equation into the expressions for the coefficients of the incident and scattered fields we obtain two matrix equations. One relating the incident wave coefficients to the coefficients of the surface field and the other relating the scattered wave coefficients to the surface field coefficients.

$$\begin{bmatrix} A_{pnm} \\ B_{pnm} \\ C_{pnm} \end{bmatrix} = -i \begin{bmatrix} (Q^{11})_{pnm}^{qij} & (Q^{12})_{pnm}^{qij} & (Q^{13})_{pnm}^{qij} \\ (Q^{21})_{pnm}^{qij} & (Q^{22})_{pnm}^{qij} & (Q^{23})_{pnm}^{qij} \\ (Q^{31})_{pnm}^{qij} & (Q^{32})_{pnm}^{qij} & (Q^{33})_{pnm}^{qij} \end{bmatrix} \begin{bmatrix} a_{qij} \\ b_{qij} \\ c_{qij} \end{bmatrix}$$

$$\begin{bmatrix} \alpha_{pnm} \\ \beta_{pnm} \\ \gamma_{pnm} \end{bmatrix} = -i \begin{bmatrix} \text{Re}(Q^{11})_{pnm}^{qij} & \text{Re}(Q^{12})_{pnm}^{qij} & \text{Re}(Q^{13})_{pnm}^{qij} \\ \text{Re}(Q^{21})_{pnm}^{qij} & \text{Re}(Q^{22})_{pnm}^{qij} & \text{Re}(Q^{23})_{pnm}^{qij} \\ \text{Re}(Q^{31})_{pnm}^{qij} & \text{Re}(Q^{32})_{pnm}^{qij} & \text{Re}(Q^{33})_{pnm}^{qij} \end{bmatrix} \begin{bmatrix} a_{qij} \\ b_{qij} \\ c_{qij} \end{bmatrix}$$

Each vector component in these equations is an infinite component vector itself. Each matrix element is an infinite dimension matrix. The  $Q^{ij}$  for the cavity problem are given by these integrals over the surface of the scattering object

$$\begin{aligned} (Q^{11})_{pnm}^{qij} &= \frac{k_s}{(\rho\omega)^2} \int d\sigma \text{Re} \tilde{\phi}_{qij}(\mathbf{r}') \cdot \hat{\mathbf{n}} \cdot [\lambda \tilde{\nabla}' \cdot \tilde{\phi}_{pnm}(\mathbf{r}') + \mu \nabla' \tilde{\phi}_{pnm}(\mathbf{r}') + \mu \tilde{\phi}_{pnm}(\mathbf{r}') \nabla'] \\ (Q^{21})_{pnm}^{qij} &= \frac{\mu k_s}{(\rho\omega)^2} \int d\sigma \text{Re} \tilde{\phi}_{qij}(\mathbf{r}') \cdot \hat{\mathbf{n}} \cdot [\nabla' \tilde{\psi}_{pnm}(\mathbf{r}') + \tilde{\psi}_{pnm}(\mathbf{r}') \nabla'] \\ (Q^{31})_{pnm}^{qij} &= \frac{\mu k_s}{(\rho\omega)^2} \int d\sigma \text{Re} \tilde{\phi}_{qij}(\mathbf{r}') \cdot \hat{\mathbf{n}} \cdot [\nabla' \tilde{\chi}_{pnm}(\mathbf{r}') + \tilde{\chi}_{pnm}(\mathbf{r}') \nabla'] \end{aligned}$$

The matrix elements  $(Q^{k2})$  are obtained by replacing  $\text{Re}\vec{\phi}_{qij}(\mathbf{r}')$  with  $\text{Re}\vec{\phi}_{qij}(\mathbf{r}')$  and  $(Q^{k3})$  are obtained by replacing  $\text{Re}\vec{\phi}_{qij}(\mathbf{r}')$  with  $\text{Re}\vec{\chi}_{qij}(\mathbf{r}')$ .  $\text{Re}(Q_{pnm}^{qij})$  is obtained by replacing the basis vectors by the corresponding regular basis vectors.

The T-matrix is obtained by solving the two matrix equations above for the coefficients of the scattered wave in terms of the coefficients of the incident wave.

$$\begin{bmatrix} a_{pnm} \\ b_{pnm} \\ c_{pnm} \end{bmatrix} = - \begin{bmatrix} (T^{11})_{pnm}^{qij} & (T^{12})_{pnm}^{qij} & (T^{13})_{pnm}^{qij} \\ (T^{21})_{pnm}^{qij} & (T^{22})_{pnm}^{qij} & (T^{23})_{pnm}^{qij} \\ (T^{31})_{pnm}^{qij} & (T^{32})_{pnm}^{qij} & (T^{33})_{pnm}^{qij} \end{bmatrix} \begin{bmatrix} A_{qij} \\ B_{qij} \\ C_{qij} \end{bmatrix}$$

The elements of the T-matrix are defined in terms of  $Q$  by the same equation as in the scalar case

$$\mathbf{T} = -\text{Re}(\mathbf{Q}^T)(\mathbf{Q}^T)^{-1}$$

As in the acoustic scattering case, the T-matrix depends only on the geometry and boundary conditions of the scatterer, not on the properties of the incident field. More complicated boundary conditions, such as those describing an elastic scatterer, are also discussed in Ref. 14.

### C. Multiple Scattering

The T-matrix approach lends itself to describing multiple scattering--the interaction of the scattered field with another obstacle. The key to treating multiple scattering is the ability to translate the origin of coordinates of the spherical basis functions. This allows one to calculate the scattering from each individual object as outlined above and then to translate the results to a common coordinate system. For multiple scattering, the scattered field of one object becomes the incident field at another. In this section, we follow Ref. 19 in discussing the application of the T-matrix to multiple scattering.

#### 1. Two Scatterers

Figure 2 shows the geometry for two scatterers  $S_1$  and  $S_2$ . There is an origin of coordinates  $O$  outside the scatterers and points  $O_1$  and  $O_2$ , located by the vectors  $\mathbf{a}_1$  and  $\mathbf{a}_2$  that serve as local origins of coordinate systems within the two scatterers. The vectors  $\mathbf{r}'_1$  and  $\mathbf{r}'_2$  are points on the surfaces  $\sigma_1$  and  $\sigma_2$  of the

scatterers relative to the O coordinate system while  $\mathbf{r}_1''$  and  $\mathbf{r}_2''$  are points on the surfaces relative to the coordinate systems within each scatterer. The vectors  $\mathbf{r}$  are observation points relative to the O system while  $\mathbf{r}_1$  and  $\mathbf{r}_2$  are observation points relative to the  $O_1$  and  $O_2$  coordinate systems.  $O_1$  and  $O_2$  are chosen so that  $\mathbf{r}_1''$  and  $\mathbf{r}_2''$  are continuous functions of spherical coordinates in their respective coordinate systems. The vectors  $\hat{\mathbf{n}}_1$  and  $\hat{\mathbf{n}}_2$  are outward normal vectors at the surface of each scatterer.

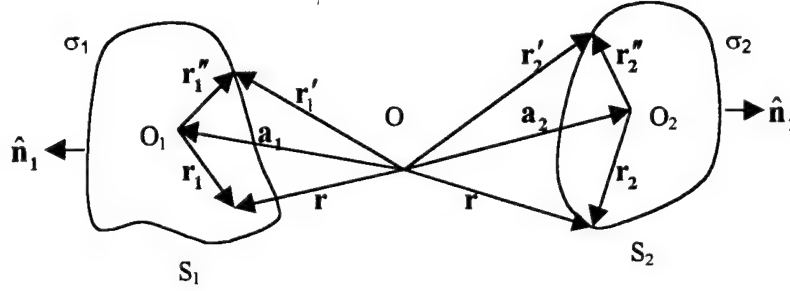


Figure 2. Geometry for a two scatterers.

In analogy with the single scatterer, we have two integral equations for the acoustic field one for  $\mathbf{r}$  outside  $S_1$  and  $S_2$

$$\Psi^s(\mathbf{r}) = \frac{1}{4\pi} \int_{S_1+S_2} d\sigma \hat{\mathbf{n}} \cdot \left[ \Psi_+(\mathbf{r}') \nabla g(k_p |\mathbf{r} - \mathbf{r}'|) - g(k_p |\mathbf{r} - \mathbf{r}'|) \nabla_+ \Psi(\mathbf{r}') \right] \quad (13)$$

and the other for  $\mathbf{r}$  inside  $S_1$  or  $S_2$

$$\Psi^i(\mathbf{r}) = -\frac{1}{4\pi} \int_{S_1+S_2} d\sigma \hat{\mathbf{n}} \cdot \left[ \Psi_+(\mathbf{r}') \nabla g(k_p |\mathbf{r} - \mathbf{r}'|) - g(k_p |\mathbf{r} - \mathbf{r}'|) \nabla_+ \Psi(\mathbf{r}') \right] \quad (14)$$

In Eqs. 13 and 14 we assumed that there are no sources inside a sphere centered at O and enclosing both scatterers. As for the acoustic scatterer above, we expand the incident field inside this sphere as

$$\Psi^i(\mathbf{r}) = \sum a_n \text{Re} \psi_n(\mathbf{r}) \quad (15)$$

To proceed we will want to expand the surface fields in Eqs. 13 and 14 in terms of regular eigenfunctions centered at  $O_1$  and  $O_2$ . We will also need to express the expansion for  $\Psi^i$  in terms of coordinates centered at  $O_1$  and  $O_2$ . As an example, consider the case for  $\mathbf{r}$  inside  $S_1$ . We use the fact that  $\mathbf{r} - \mathbf{r}'_1 = \mathbf{r}_1 - \mathbf{r}''_1$  to expand the Green's function within a sphere within  $S_1$  centered at  $O_1$ . We also restrict  $\mathbf{r}$  to those points inside  $S_1$  for which  $r_1 < r''_{\min}$  where  $r''_{\min}$  is the smallest value of  $r''$  on the surface  $\sigma_1$ . We can now identify  $r_<$  and  $r_>$  in the expansion of the Green's function to obtain

$$g(k_p|\mathbf{r} - \mathbf{r}'_1) = ik_p \sum \psi_n(k_p \mathbf{r}'') \text{Re} \psi_n(k_p \mathbf{r}_1) \quad (16)$$

We also need to expand the Green's function in the integral over  $\sigma_2$ . This is accomplished by noting that the argument of this Green's function ( $\mathbf{r} - \mathbf{r}'_2$ ) can be written as  $\mathbf{r}_1 - [\mathbf{r}''_2 - (\mathbf{a}_1 - \mathbf{a}_2)]$ . For  $r_1 < r''_{\min}$ , we have  $r_1 < |\mathbf{r}''_2 - (\mathbf{a}_1 - \mathbf{a}_2)|$ . The Green's function is

$$g(k_p|\mathbf{r} - \mathbf{r}'_2) = ik_p \sum \psi_n[k_p(\mathbf{r}''_2 - (\mathbf{a}_1 - \mathbf{a}_2))] \text{Re} \psi_n(k_p \mathbf{r}_1) \quad (17)$$

To carry out the integral over  $\sigma_1$  we need the translation properties of  $\psi_n$  and  $\text{Re} \psi_n$  to convert the arguments to the variables of integration. For  $\text{Re} \psi_n$ , noting that  $\mathbf{r} = \mathbf{r}_1 + \mathbf{a}_1$ , the translation is given by a summation over regular functions,

$$\text{Re} \psi_n(\mathbf{r}_1 + \mathbf{a}_1) = \sum_{n'} R_{nn'}(\mathbf{a}_1) \text{Re} \psi_{n'}(\mathbf{r}_1) \quad (18)$$

The translation properties of  $\psi_n$  is also given in terms of the regular eigenfunctions as

$$\psi_n[\mathbf{r}''_2 - (\mathbf{a}_1 - \mathbf{a}_2)] = \sum_{n'} \Gamma_{nn'}(-\mathbf{a}_1 + \mathbf{a}_2) \text{Re} \psi_{n'}(\mathbf{r}''_2) \quad (19)$$

This expansion is valid only for  $|\mathbf{a}_1 - \mathbf{a}_2| < r''_2$ . For the expansion inside  $S_1$  to be valid we also require  $|\mathbf{a}_1 - \mathbf{a}_2| < r''_1$ . These two conditions introduce a constraint on the configuration of scatterers that can be satisfied if the spheres defined by  $r''_1$  and  $r''_2$  do not overlap. The properties of the translation matrices  $R_{nn'}$  and  $\Gamma_{nn'}$  are given in Ref. 19.



Equations 18 and 19 can now be used in Eqs. 13 and 14 to relate the incident and scattered fields to the fields on the surface of the scatterers. The expansion coefficients of the surface fields are  $\alpha_n^i$  where  $i=1,2$  denotes the scattering object. The  $\mathbf{Q}$  matrices for each scattering object, as defined above for acoustic scattering, will also appear in the results. A superscript will identify the matrix for each scattering object as  $\mathbf{Q}^i$ . The superscript  $T$  denotes the transpose of a matrix. Equations 13 and 14 then yield the following equations in matrix notation. For  $\mathbf{r} = \mathbf{r}_1 + \mathbf{a}_1$  inside  $S_1$  with  $r_{11} < r_{11\min}$ ,

$$\mathbf{R}^T(\mathbf{a}_2)\mathbf{a} = i\mathbf{Q}^1\alpha^1 + i\Gamma(-\mathbf{a}_1 + \mathbf{a}_2)\text{Re}\mathbf{Q}^2\alpha^2 \quad (20)$$

and for  $\mathbf{r} = \mathbf{r}_2 + \mathbf{a}_2$  inside  $S_1$  with  $r_{22} < r_{22\min}$ ,

$$\mathbf{R}^T(\mathbf{a}_2)\mathbf{a} = i\Gamma(-\mathbf{a}_2 + \mathbf{a}_1)\text{Re}\mathbf{Q}^1\alpha^1 + i\mathbf{Q}^2\alpha^2 \quad (21)$$

For the region outside the scatterer we obtain an equation for the scattered field expansion coefficients.

$$\mathbf{f} = -i\mathbf{R}(\mathbf{a}_1)\text{Re}\mathbf{Q}^1\alpha^1 - i\mathbf{R}(\mathbf{a}_2)\text{Re}\mathbf{Q}^2\alpha^2 \quad (22)$$

Equations 19-21 can be used to eliminate the expansion coefficients of the field on the surface of the scatterers and obtain the T-matrix for the two scatterers  $\mathbf{T}(1,2)$ . The T-matrices of the individual scatterers,  $\mathbf{T}(i) = -\text{Re}\mathbf{Q}^i(\mathbf{Q}^i)^{-1}$ , also appear in expression for the total T-matrix. The T-matrix for two scatters is

$$\begin{aligned} \mathbf{T}(1,2) = & \mathbf{R}(\mathbf{a}_1)\left\{\mathbf{T}(1)[1 - \Gamma(-\mathbf{a}_1 + \mathbf{a}_2)\mathbf{T}(2)\Gamma(-\mathbf{a}_2 + \mathbf{a}_1)\mathbf{T}(1)]^{-1} \right. \\ & \times [1 + \Gamma(-\mathbf{a}_1 + \mathbf{a}_2)\mathbf{T}(2)\mathbf{R}(\mathbf{a}_1 - \mathbf{a}_2)]\mathbf{R}(-\mathbf{a}_1)\} \\ & + \mathbf{R}(\mathbf{a}_2)\left\{\mathbf{T}(2)[1 - \Gamma(-\mathbf{a}_2 + \mathbf{a}_1)\mathbf{T}(1)\Gamma(-\mathbf{a}_1 + \mathbf{a}_2)\mathbf{T}(2)]^{-1} \right. \\ & \times [1 + \Gamma(-\mathbf{a}_2 + \mathbf{a}_1)\mathbf{T}(1)\mathbf{R}(\mathbf{a}_2 - \mathbf{a}_1)]\mathbf{R}(-\mathbf{a}_2)\} \end{aligned} \quad (23)$$

Examination of Eq. 23 shows that it treats the two scatterers in a symmetric way. The introduction of more than one scatterer does not require more complicated surface integrals than the single scatterer case. We still need only calculate the  $\mathbf{Q}^i$  matrices of the individual scatterers. Equation 23 combines them into the T-matrix for 2 scatterers.

It is informative to examine some of the individual terms arising from Eq. 23. For  $T(1) \rightarrow 0$  we recover the single scatter result  $T(1,2) \rightarrow R(a_1)T(1)R(-a_1)$  which is the single scatter result translated from an origin inside the scattering object to one outside the object. Formally expanding the inverses in Eq. 23 yields a series that has a natural interpretation in terms of multiple scattering. The first few of these terms are interpreted in Table 1.

Expansion term	Interpretation
$T(1)$	Single scatter from 1
$T(2)$	Single scatter from 2
$T(2)\Gamma T(1)$	Scatter from 1, propagation from 1 to 2, scatter from 2
$T(1)\Gamma T(2)$	Scatter from 2, propagation from 2 to 1, scatter from 1
$T(1)\Gamma T(2)\Gamma T(1)$	Scatter from 1, propagation from 1 to 2, scatter from 2, propagation from 2 to 1, scatter from 1
$T(2)\Gamma T(1)\Gamma T(2)$	Scatter from 2, propagation from 2 to 1, scatter from 1, propagation from 1 to 2, scatter from 2

Table 1. Interpretation of terms in the expansion of  $T(1,2)$

This approach to multiple scattering is very powerful. It is a full physics approach that includes effects of energy trapping and resonances in the configuration of the scatterers.

## 2. N Scatterers

While the approach for 2 scatterers that we used above can be generalized to treat  $N$  scatterers, the resulting iterative procedures outlined in Refs. 19 and 22 are complex. Reference 23 provides a different approach that uses the "effective field" concept to develop a concise and elegant solution for the T-matrix for  $N$  scatterers. The incident field at each scatterer is expanded as

$$\Psi_j^i(\mathbf{r} - \mathbf{d}_j) = \sum_n \text{Re} \psi_n(\mathbf{r} - \mathbf{d}_j) \alpha_n^j$$

The scattered field is expanded as

$$\Psi^s(\mathbf{r}) = \sum_{j=1}^N \Psi_j^i(\mathbf{r} - \mathbf{d}_j) = \sum_{j=1}^N \sum_n \psi_n(\mathbf{r} - \mathbf{d}_j) f_n^j$$

We define the effective field incident on each scatterer as the field made up of the incident field and the fields scattered from all other obstacles. Since this is the field exterior to the scatterer under consideration, it can be expanded in terms of regular functions centered on the scatterer. The effective field incident upon the  $j^{\text{th}}$  scatterer is then

$$\begin{aligned} \Psi_j^{\text{eff}}(\mathbf{r} - \mathbf{d}_j) &= \Psi^i(\mathbf{r} - \mathbf{d}_j) + \sum_{\substack{j'=1 \\ j' \neq j}}^N \Psi^{s_j}(\mathbf{r} - \mathbf{d}_j) \\ &= \sum \text{Re} \psi_n(\mathbf{r} - \mathbf{d}_j) c_n^j \end{aligned}$$

The expansion coefficients  $f_n^j$  of the field scattered by the  $j^{\text{th}}$  object is given by the T-matrix for that scatterer as

$$f_n^j = \sum_{n'} \mathbf{T}_{nn'}^{(j)} c_{n'}^j \quad (24)$$

Expanding the expression for the effective field and using the translation matrices defined above yields

$$c_n^j = a_n^j + \sum_{\substack{j'=1 \\ j' \neq j}}^N \sum_{n'} \sum_{n''} \Gamma_{nn'}(-(\mathbf{d}_j - \mathbf{d}_{j'})) \Gamma_{n'n''}^{(j)} c_{n''}^j$$

In matrix notation this equation can be written as

$$\mathbf{c} = \mathbf{a} + \mathcal{RT}\mathbf{c} \quad (25)$$

where

$$\mathbf{c} = \begin{bmatrix} c_n^1 \\ c_n^2 \\ \dots \\ c_n^N \end{bmatrix}, \mathbf{a} = \begin{bmatrix} a_n^1 \\ a_n^2 \\ \dots \\ a_n^N \end{bmatrix}, \mathcal{T} = \begin{bmatrix} \mathbf{T}^{(1)} & 0 & \dots & 0 \\ 0 & \mathbf{T}^{(2)} & \dots & 0 \\ \dots & \dots & \dots & \dots \\ 0 & 0 & \dots & \mathbf{T}^{(N)} \end{bmatrix}$$

and

$$\mathcal{R} = \begin{bmatrix} 0 & \Gamma(-(\mathbf{d}_1 - \mathbf{d}_2)) & \Gamma(-(\mathbf{d}_1 - \mathbf{d}_2)) & \dots & \Gamma(-(\mathbf{d}_1 - \mathbf{d}_N)) \\ \Gamma(\mathbf{d}_1 - \mathbf{d}_2) & 0 & \Gamma(-(\mathbf{d}_2 - \mathbf{d}_3)) & \dots & \Gamma(-(\mathbf{d}_2 - \mathbf{d}_N)) \\ \Gamma(\mathbf{d}_1 - \mathbf{d}_3) & \Gamma(\mathbf{d}_2 - \mathbf{d}_3) & 0 & \dots & \Gamma(-(\mathbf{d}_3 - \mathbf{d}_N)) \\ \dots & \dots & \dots & \dots & \dots \\ \Gamma(\mathbf{d}_1 - \mathbf{d}_N) & \Gamma(\mathbf{d}_2 - \mathbf{d}_N) & \Gamma(\mathbf{d}_3 - \mathbf{d}_N) & \dots & 0 \end{bmatrix}$$

Using the matrix analog of Eq. 24,  $\mathbf{c} = \mathcal{T}^{-1}\mathbf{f}$ , in Eq. 25 yields the multiple-scatter T-matrix  $\mathbf{T}^{\text{MS}}$  relating the incident and scattered fields

$$\mathbf{f} = \mathbf{T}^{\text{MS}} \mathbf{a}$$

where

$$\mathbf{T}^{\text{MS}} = \mathcal{T}(\mathbf{I} - \mathcal{R}\mathcal{T})^{-1}$$

Expanding the inverse in  $\mathbf{T}^{\text{MS}}$  produces terms corresponding to increasing orders of multiple scattering

$$\mathbf{T}^{\text{MS}} = \mathcal{T} + \mathcal{T}\mathcal{R}\mathcal{T} + \mathcal{T}\mathcal{R}\mathcal{T}\mathcal{R}\mathcal{T} + \dots$$

Each  $\mathcal{T}$  matrix represents scattering by each of the  $N$  obstacles while each  $\mathcal{R}$  matrix distributes the scattered fields among the  $N$  objects. The poles of  $\mathbf{T}^{\text{MS}}$  correspond to scattering resonances of the  $N$  body system.

#### D. Layered Scatterer

The T-matrix approach has been extended to treat scattering from a structured object, such as an object made up of layers of different materials, an object with embedded scattering objects, or an object made up of non-enclosing parts. The theoretical approach we present here treats scattering from a layered object and follows the work in Ref. 24. Figure 3 shows the scattering geometry. There is a single object with two layers. A subscript  $i$ ,  $i = 1, 2$ , will be used to identify quantities in the two layers of the scatterer. A subscript 0 will denote the properties of the background medium outside the scatterers.

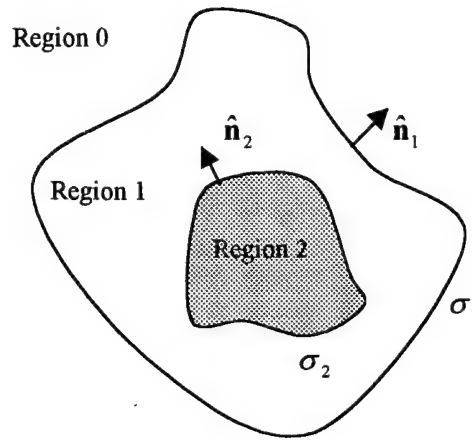


Figure 3. Geometry for a layered scatterer.

We begin by applying Huygen's principle to the region outside region 1 and using the acoustic boundary conditions of continuity of pressure and velocity to relate the field in the exterior (Region 0) to the interior (Region 1). The incident and scattered fields are expressed as

$$\Psi^i(k_0 \mathbf{r}) = \sum_n a_n \text{Re} \psi_n(k_0 \mathbf{r})$$

$$\Psi^s(k_0 \mathbf{r}) = \sum_n f_n \psi_n(k_0 \mathbf{r})$$

In the region outside  $\sigma_2$  and inside  $\sigma_1$  the field is made up of both regular (Re) and outgoing (Out) solutions and is written as

$$\Psi^1(k_1 \mathbf{r}) = \sum_n \{ \alpha_n^1 \text{Re} \psi_n(k_1 \mathbf{r}) + \beta_n^1 \psi_n(k_1 \mathbf{r}) \}$$

The integral equations yield two equations relating the coefficients of the incident and scattered fields to the coefficients of the field in Region 1

$$f_n = -i \sum_{n'} \{ Q_{nn'}^1(\text{Re}, \text{Re}) \alpha_{n'}^1 + Q_{nn'}^1(\text{Re}, \text{Out}) \beta_{n'}^1 \}$$

$$a_n = i \sum_{n'} \{ Q_{nn'}^1(\text{Out}, \text{Re}) \alpha_{n'}^1 + Q_{nn'}^1(\text{Out}, \text{Out}) \beta_{n'}^1 \}$$

where

$$Q_{nn'}^1(\text{Re}, \text{Re}) = k_0 \int_{\sigma_1} d\sigma \hat{\mathbf{n}} \cdot \left\{ \frac{\rho_1}{\rho_0} [\nabla \text{Re} \psi_n(k_0 \mathbf{r}) \text{Re} \psi_{n'}(k_1 \mathbf{r}) - \text{Re} \psi_n(k_0 \mathbf{r}) \nabla \text{Re} \psi_{n'}(k_1 \mathbf{r})] \right\}$$

The first argument (Re or Out) in  $Q_{nn'}^1$  signifies taking  $\text{Re} \psi_n$  or  $\psi_n$  as the wave functions with argument  $k_0 \mathbf{r}$  in the integral; the second argument (Re or Out) signifies taking  $\text{Re} \psi_n$  or  $\psi_n$  as the wave functions with argument  $k_1 \mathbf{r}$ .

Next, we apply Huygen's principle to the volume between  $\sigma_1$  and  $\sigma_2$ . Expressing the field inside  $\sigma_2$  as

$$\Psi^2(k_2 \mathbf{r}) = \sum_n \alpha_n^2 \text{Re} \psi_n(k_2 \mathbf{r})$$

Using the acoustic boundary conditions on surface  $\sigma_2$ , and evaluating the integrals yields two equations relating  $\alpha_n^1$ ,  $\alpha_n^2$ , and  $\beta_n^1$ .

$$-i \alpha_n^1 = \sum_{n'} Q_{nn'}^2(\text{Out}, \text{Re}) \alpha_{n'}^2$$

$$i \beta_n^1 = \sum_{n'} Q_{nn'}^2(\text{Re}, \text{Re}) \alpha_{n'}^2$$

Written in vector form, our results for the two layer scatterer are

$$\begin{aligned} \mathbf{a} &= i \left\{ \mathbf{Q}^1(\text{Out}, \text{Re}) \alpha^1 + \mathbf{Q}^1(\text{Out}, \text{Out}) \beta^1 \right\} \\ \mathbf{f} &= -i \left\{ \mathbf{Q}^1(\text{Re}, \text{Re}) \alpha^1 + \mathbf{Q}^1(\text{Re}, \text{Out}) \beta^1 \right\} \\ \alpha^1 &= i \mathbf{Q}^2(\text{Out}, \text{Re}) \alpha^2 \\ \beta^1 &= i \mathbf{Q}^2(\text{Re}, \text{Re}) \alpha^2 \end{aligned}$$

Solving these for the relation between  $\mathbf{a}$  and  $\mathbf{f}$  yields the T-matrix for a two-layered scatterer

$$\mathbf{T}^{1,2} = \left\{ \mathbf{T}^1 - \mathbf{Q}^1(\text{Re}, \text{Out}) \mathbf{T}^2 \left[ \mathbf{Q}^1(\text{Out}, \text{Re}) \right]^{-1} \right\} \left\{ 1 + \mathbf{Q}^1(\text{Out}, \text{Out}) \mathbf{T}^2 \left[ \mathbf{Q}^1(\text{Out}, \text{Re}) \right]^{-1} \right\}^{-1}$$

where

$$\mathbf{T}^i = -\mathbf{Q}^i(\text{Re}, \text{Re}) \left[ \mathbf{Q}^i(\text{Out}, \text{Re}) \right]^{-1}$$

is the T-matrix of a non-layered scatterer bounded by surface  $\sigma_i$  and having the material properties of Region  $i$ .

Reference 24 give a recursive approach for calculating the T-matrix of an N layer scatterer. The T-matrix for a scatterer formed by removing the first  $j$  layers of an N layer scatterer layers  $\mathbf{T}^{j+1, \dots, N}$  is given by

$$\begin{aligned} \mathbf{T}^{j+1, \dots, N} &= \left\{ \mathbf{T}^{j+1} - \mathbf{Q}^{j+1}(\text{Re}, \text{Out}) \mathbf{T}^{j+2, \dots, N} \left[ \mathbf{Q}^{j+1}(\text{Out}, \text{Re}) \right]^{-1} \right. \\ &\quad \times \left. \left\{ 1 + \mathbf{Q}^{j+1}(\text{Out}, \text{Out}) \mathbf{T}^{j+2, \dots, N} \left[ \mathbf{Q}^{j+1}(\text{Out}, \text{Re}) \right]^{-1} \right\} \right\} \end{aligned}$$

which can be constructed by working from the innermost layer out to the surface.

#### E. Inhomogeneous Scatterer

Scattering from an object with continuously varying properties can be treated within the T-matrix formalism, but general results cannot be given. The difficulty is that the fields in the interior of the object cannot be expanded in terms of spherical wave functions since they may not be solutions to the wave equation for the interior of the scattering object<sup>39</sup>. A basis set must be defined for each

type of inhomogeneity. Once the basis set is known, the rest of the T-matrix formalism follows.

#### F. Scattering from highly non-spherical shapes

The development of T-matrix theory that we have presented uses spherical coordinates and basis functions and works well for scattering objects that are nearly spherical. There is, however, no fundamental restriction to treating objects with more complicated shapes. The theory itself places minimal restrictions on the shape of the scatterer. The surface of the scatterer must be continuous and described by a single valued function of spherical coordinates. Scattering from nearly cylindrical objects can be treated using cylindrical coordinates and basis functions. We will not discuss cylindrical coordinates since the theory follows that for spherical coordinates very closely. In this section we discuss scattering from highly non-spherical objects such as prolate and oblate spheroids of high aspect ratio.

The results presented above can be used directly, provided we know how to describe the surface element in the integral equations for the Q matrix. For a spheroidal (prolate or oblate) scatterer, the surface element is<sup>28</sup>

$$\hat{n}(\theta)d\sigma = \left( \hat{e}_r - \frac{\hat{e}_\theta}{r} \frac{dr(\theta)}{d\theta} \right) r^2 \sin\theta d\theta d\phi$$

where:  $a$  and  $b$  are the semi-major and semi-minor axes of the spheroid, and

$$r(\theta) = \left( \frac{\cos^2\theta}{a^2} + \frac{\sin^2\theta}{b^2} \right)^{-1/2}$$

For a prolate spheroid (cigar shape)  $a > b$ ; for an oblate spheroid (pancake shape)  $a < b$ ; and for a sphere,  $a = b$ .

For objects with large aspect ratios ( $a \gg b$  or  $a \ll b$ ) there are practical problems in applying the T-matrix approach. Larger numbers of terms in the approximation of the infinite dimensional Q matrix are needed for convergence and the matrices become ill conditioned. Techniques for dealing with the ill conditioned matrix problem have been developed<sup>10,30</sup> but will not be discussed here.



Reference 29 discusses a fundamentally different approach to applying the T-matrix formalism to large aspect ratio scatterers. The idea is to use a coordinate system that closely approximates the shape of the scatterer to reduce the number of terms needed to approximate the matrices and reduce the severity of the ill conditioned matrix problem. This approach is novel since it is well known that the vector wave equation is separable only in Cartesian, cylindrical, and spherical coordinates.<sup>40</sup> An analytic Green's tensor, which is used to construct the T-matrix, cannot be formulated in other coordinate systems since the vector basis functions are not orthogonal. Reference 29 avoids this problem by developing a Huygen's principle based on Betti's third identity<sup>41</sup> that does not require the Green's tensor. They use spheroidal vector basis functions that contain the spheroidal counterparts to the spherical Hankel functions and spherical harmonics. This approach is outlined below.

Betti's identity states that if  $\mathbf{u}$  and  $\mathbf{v}$  are solutions to the time independent vector Helmholtz equation in the volume, and  $\tilde{\mathbf{T}}(\mathbf{u})$  and  $\tilde{\mathbf{T}}(\mathbf{v})$  are the stress tensors associated with  $\mathbf{u}$  and  $\mathbf{v}$ , then

$$\int d\sigma \hat{\mathbf{n}} \cdot [\tilde{\mathbf{T}}(\mathbf{u}) \cdot \mathbf{v} - \tilde{\mathbf{T}}(\mathbf{v}) \cdot \mathbf{u}] = 0$$

where the integral is over the surface bounding a volume and  $\hat{\mathbf{n}}$  is a unit vector pointing out of the volume and normal to the surface.

Huygen's principle is obtained by using expressions for  $\mathbf{u}$  and  $\mathbf{v}$  which describe the scattering process. We bound the scattering object on the outside by the smallest spheroid  $S_+$  containing the scatterer and on the inside by the largest spheroid  $S_-$  contained by the scatterer. Using the spheroidal basis functions (given in Ref. 29) we expand the incident wave  $\mathbf{u}^i$ , the scattered wave  $\mathbf{u}^s$ , and the wave inside  $S_-$   $\mathbf{u}^r$  as

$$\begin{aligned}\mathbf{u}^i &= \sum_n a_n \text{Re} \tilde{\psi}_n \\ \mathbf{u}^s &= \sum_n f_n \tilde{\psi}_n \\ \mathbf{u}^r &= \sum_n \alpha_n \text{Re} \tilde{\psi}_n^0\end{aligned}$$

where  $\tilde{\psi}_n$  are the spheroidal vector basis functions. The superscript 0 indicates that the properties of the scatterer rather than the background medium are used.

For the surface bounded by  $S$ , the surface of the scattering object, and  $S_+$ , we have

$$\int_{S_+} d\sigma \hat{n} \cdot [\tilde{T}(u) \cdot v - \tilde{T}(v) \cdot u] = \int_S d\sigma \hat{n} \cdot [\tilde{T}(u) \cdot v - \tilde{T}(v) \cdot u]$$

On  $S_+$  we have

$$\begin{aligned} u &= \sum_n a_n \text{Re} \tilde{\psi}_n + \sum_n f_n \tilde{\psi}_n \\ t(u) &= \sum_n a_n t(\text{Re} \tilde{\psi}_n) + \sum_n f_n t(\tilde{\psi}_n) \end{aligned}$$

where  $t = \hat{n} \cdot \tilde{T}$  is the traction. Choosing  $v = \tilde{\psi}_n$  and  $v = \text{Re} \tilde{\psi}_n$  and substituting above results into the two equations yields

$$\begin{aligned} -i \sum_{n'} O_{n'n} a_{n'} &= \int_S d\sigma [t_+(u) \cdot \tilde{\psi}_n - t(\tilde{\psi}_n) \cdot u_+] \\ i \sum_{n'} O_{n'n} f_{n'} &= \int_S d\sigma [t_+(u) \cdot \text{Re} \tilde{\psi}_n - t(\text{Re} \tilde{\psi}_n) \cdot u_+] \end{aligned}$$

where  $t_+$  and  $u_+$  are the traction and displacement on outside surface of the scatterer. The matrix elements  $O_{n'n}$  are related to the orthogonality and normalization of the spheroidal harmonics.

We now apply the boundary conditions for two solids in contact at the surface of the scatterer:  $t_+ = t_-$  and  $u_+ = u_-$ . Replacing the quantities on the outside of the scatterer with those on the inside in the equations for the incident and scattered wave coefficients results in

$$\begin{aligned} -i \sum_{n'} O_{n'n} a_{n'} &= \int_S d\sigma [t_-(u) \cdot \tilde{\psi}_n - t(\tilde{\psi}_n) \cdot u_-] \\ i \sum_{n'} O_{n'n} f_{n'} &= \int_S d\sigma [t_-(u) \cdot \text{Re} \tilde{\psi}_n - t(\text{Re} \tilde{\psi}_n) \cdot u_-] \end{aligned}$$

We next expand the surface traction and displacement in term of the spheroidal basis functions for the interior of the scatterer.

$$\mathbf{u}_- = \sum_n b_n \text{Re} \bar{\psi}_n^0$$

$$\mathbf{t}_- = \sum_n b_n \mathbf{t}(\text{Re} \bar{\psi}_n^0)$$

Substituting these expansions into the integral equations and using

$$R_{nn'} = \int_S d\sigma [\mathbf{t}(\text{Re} \bar{\psi}_{n'}) \cdot \bar{\psi}_n - \mathbf{t}(\bar{\psi}_n) \cdot \text{Re} \bar{\psi}_{n'}]$$

$$\text{Re} R_{nn'} = \int_S d\sigma [\mathbf{t}(\text{Re} \bar{\psi}_{n'}) \cdot \text{Re} \bar{\psi}_n - \mathbf{t}(\text{Re} \bar{\psi}_n) \cdot \text{Re} \bar{\psi}_{n'}]$$

we find

$$-i \sum_{n'} O_{n'n} a_{n'} = \sum_{n'} R_{nn'} b_{n'}$$

$$i \sum_{n'} O_{n'n} f_{n'} = \sum_{n'} \text{Re} R_{nn'} b_{n'}$$

Since the matrix  $\mathbf{O}$  is symmetric, we arrive at the T-matrix for a spheroidal system

$$\mathbf{T} = -\text{Re} \mathbf{Q} (\mathbf{Q})^{-1}$$

$$\mathbf{Q} = \mathbf{O}^{-1} \mathbf{R}$$

$$\text{Re} \mathbf{Q} = \mathbf{O}^{-1} \text{Re} \mathbf{R}$$

The T-matrix for the spheroidal system differs from that for a spherical system by the inclusion of the  $\mathbf{O}$  matrices. The non-diagonal nature of  $\mathbf{O}$  arises from the mode coupling in geometries other than spherical.

### G. Buried scatterers

For application to scattering from objects buried in the seafloor, we need to know how to use the T-matrix for a scatterer buried in a half-space. In this section we follow the presentation given in Ref. 33.

#### 3. Preliminaries

Figure 4 shows the geometry we will consider. There are three acoustic media in the volumes  $V_0$ ,  $V_1$ , and  $V_2$ . The media have densities  $\rho_i$ , velocities  $c_i$ , and wave functions  $\Psi_i$ , where  $i=1, 2$ , and  $3$  indicate the media. The surface  $\sigma_1$  encloses the scatterer located below the two-dimensional surface  $\sigma_0$  separating volumes  $V_0$  and  $V_1$ . The surface  $\sigma_0$  has an average depth of  $z = 0$  and is confined between two planes with constant  $z$  coordinates indicated by the dashed lines. The point  $P$  is the source location in volume  $V_0$ .

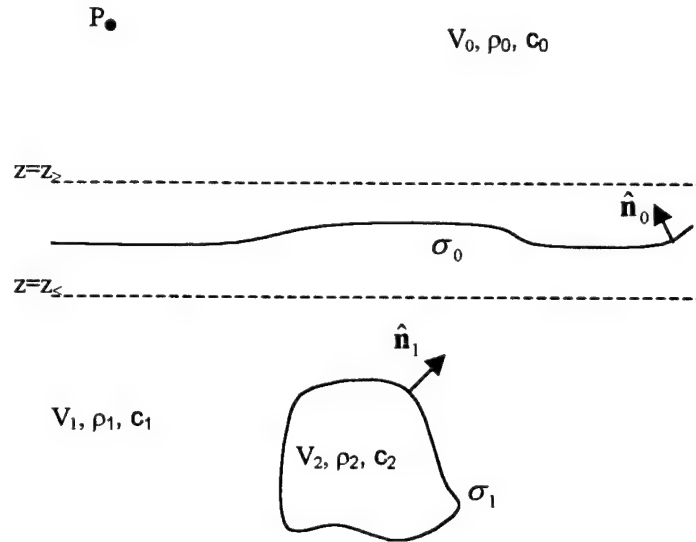


Figure 4. Geometry for a buried scatterer.

We assume that the wave field is harmonic and generated by a point source at  $P$  in  $V_0$ . The wave fields in each of the media satisfy

$$(\nabla^2 + k_r^2)\Psi_r = 0, \quad r = 1, 2, 3$$

where  $k_r = \omega/c_r$  is the wavenumber of medium  $r$ .

We begin by considering the integral equations for a surface bounded by a finite part of  $\sigma_0$  and half of a sphere into the lower half plane. Letting the radius of the sphere go to infinity we obtain:

$$\begin{aligned}\Psi_0(\mathbf{r}) &= \Psi_0^i(\mathbf{r}) + \int_{\sigma_0} d\sigma' \hat{\mathbf{n}}_0 \cdot [\Psi_0^+(\mathbf{r}') \nabla' g(k_0|\mathbf{r}-\mathbf{r}') - g(k_0|\mathbf{r}-\mathbf{r}') \nabla' \Psi_0^+(\mathbf{r}')] \quad \text{for } \mathbf{r} \text{ in } V_0 \\ 0 &= \Psi_0^i(\mathbf{r}) + \int_{\sigma_0} d\sigma' \hat{\mathbf{n}}_0 \cdot [\Psi_0^+(\mathbf{r}') \nabla' g(k_0|\mathbf{r}-\mathbf{r}') - g(k_0|\mathbf{r}-\mathbf{r}') \nabla' \Psi_0^+(\mathbf{r}')] \quad \text{for } \mathbf{r} \text{ outside } V_0\end{aligned}\quad (26)$$

where  $\Psi_0^+$  is the field on  $\sigma_0$  as it is approached from above. For this problem we will use an expansion of the free space Green's function in terms of plane wave traveling away from  $\sigma_0$  instead of the spherical wave expansion used above. By restricting the region of  $V_0$  that we consider to those  $\mathbf{r}$  for which  $z > z_0$  and the region outside of  $V_0$  to those  $\mathbf{r}$  for which  $z < z_0$ , we can use the following expansion for the Green's function in both integrals.

$$g(k_0|\mathbf{r}-\mathbf{r}') = \frac{ik_0}{8\pi^2} \int_0^{2\pi} d\phi \int_{C_{\pm}} d\theta \sin(\theta) e^{ik_0 \cdot (\mathbf{r}-\mathbf{r}')}$$

$\hat{\mathbf{k}}_0 = \mathbf{k}_0/k_0$  where:  $\mathbf{k}_0 = k_0(\sin \theta \cos \phi, \sin \theta \sin \phi, \cos \theta)$ ,  $\theta$  and  $\phi$  are the polar and azimuthal angles giving the spherical coordinates of the unit vector  $\hat{\mathbf{k}}_0 = \mathbf{k}_0/k_0$ . The integration is over contour  $C_+$  for  $z > z_0$  (propagation upward) and over  $C_-$  for  $z < z_0$  (propagation downward). The contours are shown in Fig. 5.

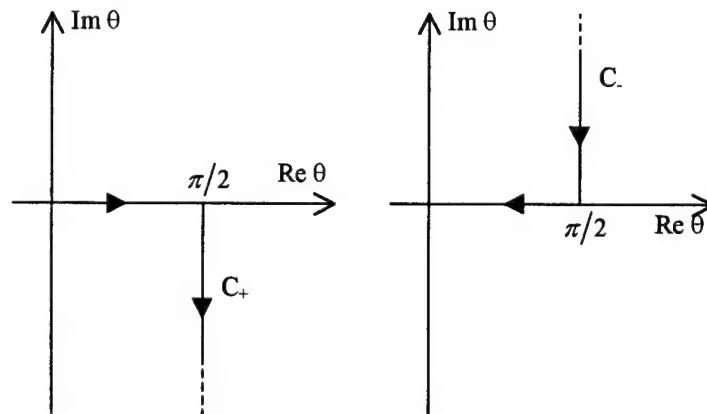


Figure 5. Integration contours.

#### 4. Integral Equations for the Surface $\sigma_0$

In this section we obtain integral equations linking the incident field and the field scattered from the plane surface. Using Eq. 26 for  $\mathbf{r}$  in  $V_0$  and the expansion of the Green's function in terms of plane waves, the scattered field in the region above  $z_p$  can be written as

$$\Psi_0^s(\mathbf{r}) = \int_0^{2\pi} d\phi_0 \int_{C_+} d\theta_0 f(\mathbf{k}_0) e^{i\mathbf{k}_0 \cdot \mathbf{r}} \sin \theta_0$$

where

$$f(\mathbf{k}_0) = \frac{ik_0}{8\pi} \int_{\sigma_0} d\sigma'_0 \hat{\mathbf{n}}_0 \cdot [\Psi_0^+(\mathbf{r}') \nabla'(e^{-i\mathbf{k}_0 \cdot \mathbf{r}'}) - e^{-i\mathbf{k}_0 \cdot \mathbf{r}'} \nabla' \Psi_0^+(\mathbf{r}')] \quad \hat{\mathbf{k}}_0 \in C_+ \quad (27)$$

We next use Eq. 26 for  $\mathbf{r}$  outside  $V_0$  to obtain an expression linking the incident field to the fields on the surface. The incident field emanating from a point source located at  $\mathbf{r}_p$  in  $V_0$  above  $z_p$  is expressed first in terms of spherical wave basis functions as

$$\Psi_0^i(\mathbf{r}) = \sum_n a_n \psi_n[k_0(\mathbf{r} - \mathbf{r}_p)]$$

where the subscript  $n$  refers to the subscript set  $pnm$  used in previous sections. For  $z > z_p$  and  $z < z_p$  the spherical wave functions can be expanded in terms of plane waves as<sup>40</sup>

$$\psi_n(k\mathbf{r}) = \frac{1}{2\pi i^n} \int_0^{2\pi} d\phi \int_{C_\pm} d\theta Y_n(\hat{\mathbf{k}}) e^{i\mathbf{k} \cdot \mathbf{r}} \sin \theta$$

where the contour is over  $C_+$  for  $z > 0$  and over  $C_-$  for  $z < 0$ . For  $z < z_p$  the expression for the incident field in terms of the plane wave expansion is

$$\Psi_0^i(\mathbf{r}) = \int_0^{2\pi} d\phi_0 \int_{C_-} d\theta_0 a(\mathbf{k}_0) e^{i\mathbf{k}_0 \cdot \mathbf{r}} \sin \theta_0$$

We now use Eq. 26 for  $\mathbf{r}$  outside  $V_0$  to obtain

$$a(\mathbf{k}_0) = -\frac{ik_0}{8\pi} \int_{\sigma_0} d\sigma'_0 \hat{\mathbf{n}}_0 \cdot [\Psi_0^+(\mathbf{r}') \nabla' (e^{-i\mathbf{k}_0 \cdot \mathbf{r}'} - e^{-i\mathbf{k}_0 \cdot \mathbf{r}'} \nabla' \Psi_0^+(\mathbf{r}'))] \quad \hat{\mathbf{k}}_0 \in C_- \quad (28)$$

The only difference in the integrals for  $f(\mathbf{k}_0)$  and  $a(\mathbf{k}_0)$  is that the plane wave expansions refer to upward propagating waves ( $\hat{\mathbf{k}}_0 \in C_+$ ) for  $f(\mathbf{k}_0)$  and downward propagating waves ( $\hat{\mathbf{k}}_0 \in C_-$ ) for  $a(\mathbf{k}_0)$ .

## 5. Surface Fields

We will now use the integral equations based on the surface bounding medium 1 to remove the surface fields from the expressions for  $f(\mathbf{k}_0)$  and  $a(\mathbf{k}_0)$ . The surfaces  $\sigma_0$  and  $\sigma_1$  enclose  $V_1$ . Since there are no sources in  $V_1$ , the integral equations for this surface are

$$\begin{aligned} \Psi_1(\mathbf{r}) &= -\int_{\sigma_0} d\sigma' \hat{\mathbf{n}}_0 \cdot [\Psi_1^-(\mathbf{r}') \nabla' g(k_1|\mathbf{r}-\mathbf{r}') - g(k_1|\mathbf{r}-\mathbf{r}') \nabla' \Psi_1^-(\mathbf{r}')] \quad \text{for } \mathbf{r} \text{ in } V_1 \\ &\quad + \int_{\sigma_1} d\sigma' \hat{\mathbf{n}}_1 \cdot [\Psi_1^+(\mathbf{r}') \nabla' g(k_1|\mathbf{r}-\mathbf{r}') - g(k_1|\mathbf{r}-\mathbf{r}') \nabla' \Psi_1^+(\mathbf{r}')] \\ 0 &= -\int_{\sigma_0} d\sigma' \hat{\mathbf{n}}_0 \cdot [\Psi_1^-(\mathbf{r}') \nabla' g(k_1|\mathbf{r}-\mathbf{r}') - g(k_1|\mathbf{r}-\mathbf{r}') \nabla' \Psi_1^-(\mathbf{r}')] \quad \text{for } \mathbf{r} \text{ in } V_0 \text{ or } V_2 \\ &\quad + \int_{\sigma_1} d\sigma' \hat{\mathbf{n}}_1 \cdot [\Psi_1^+(\mathbf{r}') \nabla' g(k_1|\mathbf{r}-\mathbf{r}') - g(k_1|\mathbf{r}-\mathbf{r}') \nabla' \Psi_1^+(\mathbf{r}')] \end{aligned} \quad (29)$$

The boundary conditions on  $\sigma_0$  and  $\sigma_1$  will be used to relate the surface fields  $\Psi_1^\pm$  to the surface fields  $\Psi_0^+$  and  $\Psi_2^-$ . To eliminate  $\Psi_1^+$  we use two forms of Eq. 29, one for  $\mathbf{r}$  in  $V_0$  and the other for  $\mathbf{r}$  in  $V_2$ .

For  $\mathbf{r}$  in  $V_0$ , the T-matrix based on spherical waves gives the effect of the scatterer bounded by  $\sigma_1$ . The appropriate Green's function for the integral over

$\sigma_1$  is given by the expansion in spherical basis functions as used in the previous sections,

$$g(k_1|\mathbf{r}-\mathbf{r}') = ik_1 \sum \text{Re} \psi_n(k_1 \mathbf{r}_<) \psi_n(k_1 \mathbf{r}_>)$$

To enable a consistent definition of  $\mathbf{r}_<$  and  $\mathbf{r}_>$  for the integral over  $\sigma_1$ , we restrict  $\mathbf{r}$  to the exterior of a sphere with a center inside  $\sigma_1$  and enclosing  $\sigma_1$ . Then for the integral over the surface of  $\sigma_1$ , we have  $\mathbf{r}_> = \mathbf{r}$  and  $\mathbf{r}_< = \mathbf{r}'$ . Equation 29 for  $\mathbf{r}$  in  $V_0$  is then

$$\begin{aligned} & \int_{\sigma_0} d\sigma' \hat{\mathbf{n}}_0 \cdot [\Psi_1^-(\mathbf{r}') \nabla' g(k_1|\mathbf{r}-\mathbf{r}') - g(k_1|\mathbf{r}-\mathbf{r}') \nabla' \Psi_1^-(\mathbf{r}')] \\ &= ik_1 \sum_n \psi_n(k_1 \mathbf{r}) \int_{\sigma_1} d\sigma' \hat{\mathbf{n}}_1 \cdot [\Psi_1^+(\mathbf{r}') \nabla' \text{Re} \psi_n(k_1 \mathbf{r}') - \text{Re} \psi_n(k_1 \mathbf{r}') \nabla' \Psi_1^+(\mathbf{r}')] \end{aligned} \quad (30)$$

Similarly, by restricting  $\mathbf{r}$  to the interior of a sphere with a center inside  $\sigma_1$  and enclosed by  $\sigma_1$  we have  $\mathbf{r}_> = \mathbf{r}'$  and  $\mathbf{r}_< = \mathbf{r}$ . We then have for  $\mathbf{r}$  in  $V_2$

$$\begin{aligned} & \int_{\sigma_0} d\sigma' \hat{\mathbf{n}}_0 \cdot [\Psi_1^-(\mathbf{r}') \nabla' g(k_1|\mathbf{r}-\mathbf{r}') - g(k_1|\mathbf{r}-\mathbf{r}') \nabla' \Psi_1^-(\mathbf{r}')] \\ &= ik_1 \sum_n \text{Re} \psi_n(k_1 \mathbf{r}) \int_{\sigma_1} d\sigma' \hat{\mathbf{n}}_1 \cdot [\Psi_1^+(\mathbf{r}') \nabla' \psi_n(k_1 \mathbf{r}') - \psi_n(k_1 \mathbf{r}') \nabla' \Psi_1^+(\mathbf{r}')] \end{aligned} \quad (31)$$

We next use the boundary conditions to eliminate  $\Psi_1^+$  in the above two equations. Since we want to describe the scattering object in terms of its T-matrix, we first expand the surface field inside the scatterer we expand in regular basis functions and obtain

$$\Psi_2^-(\mathbf{r}) = \sum \alpha_n^{(2)} \text{Re} \psi_n(k_2 \mathbf{r})$$



For the field in volume  $V_1$ , we use the plane wave expansion containing both waves propagating both upward and downward. This corresponds to both integration contours and results in

$$\Psi_1^-(\mathbf{r}) = \int_0^{2\pi} d\phi_1 \left[ \int_{C_-} d\theta_1 \alpha(\mathbf{k}_1) e^{i\mathbf{k}_1 \cdot \mathbf{r}} \sin \theta_1 + \int_{C_+} d\theta_1 \beta(\mathbf{k}_1) e^{i\mathbf{k}_1 \cdot \mathbf{r}} \sin \theta_1 \right]$$

Using the acoustic boundary conditions on  $\sigma_1$ , Eq. 30 for  $\mathbf{r}$  in  $V_0$  becomes

$$\begin{aligned} & \int_0^{2\pi} d\phi_1 \left[ \int_{C_-} d\theta_1 \alpha(\mathbf{k}_1) I(\mathbf{k}_1, \mathbf{r}) \sin \theta_1 + \int_{C_+} d\theta_1 \beta(\mathbf{k}_1) I(\mathbf{k}_1, \mathbf{r}) \sin \theta_1 \right] \\ &= -i \sum_{nn'} \psi_n(k_1 \mathbf{r}) Q_{nn'}(\text{Re}, \text{Re}) \alpha_n^{(2)} \end{aligned} \quad (32)$$

and Eq. 31 for  $\mathbf{r}$  in  $V_2$  becomes

$$\begin{aligned} & \int_0^{2\pi} d\phi_1 \left[ \int_{C_-} d\theta_1 \alpha(\mathbf{k}_1) I(\mathbf{k}_1, \mathbf{r}) \sin \theta_1 + \int_{C_+} d\theta_1 \beta(\mathbf{k}_1) I(\mathbf{k}_1, \mathbf{r}) \sin \theta_1 \right] \\ &= -i \sum_{nn'} \psi_n(k_1 \mathbf{r}) Q_{nn'}(\text{Out}, \text{Re}) \alpha_n^{(2)} \end{aligned} \quad (33)$$

We note that Eqs. 32 and 33 differ in two ways. First, the arguments of the  $Q$  matrices are different. Second, the field points  $\mathbf{r}$  are different. For Eq. 32,  $\mathbf{r}$  is in  $V_0$  while for Eq. 33  $\mathbf{r}$  is in  $V_2$ .

The  $Q$  matrices are defined by

$$\begin{aligned} Q_{nn'}(\text{Re}, \text{Re}) &= k_1 \int_{\sigma_1} d\sigma' \hat{\mathbf{n}}_1 \cdot \left\{ \text{Re} \psi_n(k_1 \mathbf{r}') \nabla' \text{Re} \psi_{n'}(k_2 \mathbf{r}') - \frac{\rho_2}{\rho_1} [\nabla' \text{Re} \psi_n(k_1 \mathbf{r}')] \text{Re} \psi_{n'}(k_2 \mathbf{r}') \right\} \\ Q_{nn'}(\text{Out}, \text{Re}) &= k_1 \int_{\sigma_1} d\sigma' \hat{\mathbf{n}}_1 \cdot \left\{ \psi_n(k_1 \mathbf{r}') \nabla' \text{Re} \psi_{n'}(k_2 \mathbf{r}') - \frac{\rho_2}{\rho_1} [\nabla' \psi_n(k_1 \mathbf{r}')] \text{Re} \psi_{n'}(k_2 \mathbf{r}') \right\} \end{aligned}$$

and  $I(\mathbf{k}, \mathbf{r})$  is given by

$$I(\mathbf{k}, \mathbf{r}) = \int_{\sigma_0} d\sigma' \hat{\mathbf{n}}_0 \cdot \left[ e^{i\mathbf{k} \cdot \mathbf{r}'} \nabla' g(k_1 |\mathbf{r} - \mathbf{r}'|) - (\nabla' e^{i\mathbf{k} \cdot \mathbf{r}'}) g(k_1 |\mathbf{r} - \mathbf{r}'|) \right]$$

The value of  $I(\mathbf{k}, \mathbf{r})$  depends on whether  $\hat{\mathbf{k}}$  is on contour  $C_+$  or  $C_-$  and on whether  $\mathbf{r}$  is above or below  $\sigma_0$ . Evaluating  $I(\mathbf{k}, \mathbf{r})$  yields

$$I(\mathbf{k}, \mathbf{r}) = \begin{cases} e^{i\mathbf{k} \cdot \mathbf{r}} & \text{for } \hat{\mathbf{k}} \in C_+ \\ 0 & \text{for } \hat{\mathbf{k}} \in C_- \end{cases} \text{ for } \mathbf{r} \text{ above } \sigma_0$$

$$I(\mathbf{k}, \mathbf{r}) = \begin{cases} 0 & \text{for } \hat{\mathbf{k}} \in C_+ \\ -e^{i\mathbf{k} \cdot \mathbf{r}} & \text{for } \hat{\mathbf{k}} \in C_- \end{cases} \text{ for } \mathbf{r} \text{ below } \sigma_0$$

Using these values for  $I(\mathbf{k}, \mathbf{r})$  Eqs. 32 and 33 become

$$\int_0^{2\pi} d\phi_1 \int_{C_+} d\theta_1 \beta(\mathbf{k}_1) (e^{i\mathbf{k}_1 \cdot \mathbf{r}}) \sin \theta_1 = -i \sum_{nn'} \psi_n(k_1 \mathbf{r}) Q_{nn'}(\text{Re}, \text{Re}) \alpha_n^{(2)} \quad \text{for } \mathbf{r} \text{ in } V_0 \quad (34)$$

$$\int_0^{2\pi} d\phi_1 \int_{C_-} d\theta_1 \alpha(\mathbf{k}_1) (-e^{i\mathbf{k}_1 \cdot \mathbf{r}}) \sin \theta_1 = -i \sum_{nn'} \psi_n(k_1 \mathbf{r}) Q_{nn'}(\text{Out}, \text{Re}) \alpha_n^{(2)} \quad \text{for } \mathbf{r} \text{ in } V_2 \quad (35)$$

We now introduce a quantity  $Q(\mathbf{k}_0, \mathbf{k}_1)$  for scattering of plane waves from the surface  $\sigma_0$  that is analogous to the  $Q$  matrix for scattering from a bounded scatterer.

$$Q(\mathbf{k}_0, \mathbf{k}_1) = \frac{k_0}{8\pi} \int_{\sigma_0} d\sigma' \hat{\mathbf{n}}_0 \cdot \left[ e^{-i\mathbf{k}_0 \cdot \mathbf{r}'} \nabla' (e^{-i\mathbf{k}_1 \cdot \mathbf{r}'}) - \frac{\rho_1}{\rho_0} \nabla' (e^{-i\mathbf{k}_0 \cdot \mathbf{r}'}) e^{-i\mathbf{k}_1 \cdot \mathbf{r}'} \right]$$

The value of  $Q(\mathbf{k}_0, \mathbf{k}_1)$  depends on the contour used for  $\hat{\mathbf{k}}_0$  and  $\hat{\mathbf{k}}_1$ .

Using the plane wave expansion for  $\Psi_1^-$  and  $Q(\mathbf{k}_0, \mathbf{k}_1)$ , Eqs. 27 and 28 for  $f(\mathbf{k}_0)$  and  $\alpha(\mathbf{k}_0)$  become

$$f(\mathbf{k}_0) = -i \int_0^{2\pi} d\phi_1 \left[ \int_{C_-} d\theta_1 \alpha(\mathbf{k}_1) Q(\mathbf{k}_0, \mathbf{k}_1) \sin \theta_1 + \int_{C_+} d\theta_1 \beta(\mathbf{k}_1) Q(\mathbf{k}_0, \mathbf{k}_1) \sin \theta_1 \right] \hat{\mathbf{k}}_0 \in C_+ \quad (36)$$

$$a(\mathbf{k}_0) = i \int_0^{2\pi} d\phi_1 \left[ \int_{C_-} d\theta_1 \alpha(\mathbf{k}_1) Q(\mathbf{k}_0, \mathbf{k}_1) \sin \theta_1 + \int_{C_+} d\theta_1 \beta(\mathbf{k}_1) Q(\mathbf{k}_0, \mathbf{k}_1) \sin \theta_1 \right] \hat{\mathbf{k}}_0 \in C_- \quad (37)$$

## 6. T-matrix for the Buried Scatterer

Equations 34 and 35 involve expansions using two different basis sets. The left side of these equations is an expansion in plane waves while the right sides are expansions in spherical harmonics. These equations are further manipulated and used to express the relationship between  $\alpha(\mathbf{k}_1)$  and  $\beta(\mathbf{k}_1)$  in terms of the T-matrix for the scattering object. First we manipulate Eq. 35 into a relationship based on the spherical wave function basis set. Multiplying each side by the spherical harmonic  $Y_m(\hat{\mathbf{r}})$ , integrating over the unit sphere, and using the plane wave expansion of the spherical wave functions on the unit sphere

$$j_m(kr) Y_m(\hat{\mathbf{r}}) = \frac{1}{4\pi i^m} \int_0^{2\pi} d\phi \int_0^\pi d\vartheta e^{i\mathbf{k}\cdot\mathbf{r}} Y_m(\hat{\mathbf{r}}) \sin \vartheta$$

yields

$$\begin{aligned} & -4\pi i^m j_m(kr) \int_0^{2\pi} d\phi_1 \int_{C_-} d\theta_1 \alpha(\mathbf{k}_1) Y_m(\hat{\mathbf{k}}_1) \sin \theta_1 \\ & = -i \sum_{nn'} j_n(k_1 r) \left[ \int_0^{2\pi} d\phi \int_0^\pi d\vartheta Y_m(\hat{\mathbf{r}}) Y_n(\hat{\mathbf{r}}) \sin \vartheta \right] Q_{nn'}(\text{Out, Re}) \alpha_{n'}^{(2)} \end{aligned}$$

The quantity in brackets above is the orthogonality integral for spherical harmonics and is  $\delta_{n,m}$ . Using this we have

$$4\pi i^n \int_0^{2\pi} d\phi_1 \int_{C_-} d\theta_1 \alpha(\mathbf{k}_1) Y_n(\hat{\mathbf{k}}_1) \sin \theta_1 = i \sum_{n'} Q_{nn'}(\text{Out, Re}) \alpha_{n'}^{(2)} \quad (38)$$

Equation 34 can be similarly manipulated to give a relationship between plane wave amplitudes. By considering  $\mathbf{r}$  on a plane of constant  $z = z_0 > z_>$  we can use the plane wave expansion on contour  $C_+$  for  $\psi_n(k_1 \mathbf{r})$  and obtain

$$\begin{aligned} & \int_0^{2\pi} d\phi_1 \int_{C_+} d\theta_1 \beta(\mathbf{k}_1) (e^{ik_1 \cdot \mathbf{r}}) \sin \theta_1 \\ &= -i \sum_{nn'} \frac{1}{2\pi i^{n+1}} \int_0^{2\pi} d\phi_1 \int_{C_+} d\theta_1 Y_n(\hat{\mathbf{k}}_1) e^{ik_1 \cdot \mathbf{r}} \sin \theta_1 Q_{nn'}(\text{Re}, \text{Re}) \alpha_n^{(2)} \end{aligned}$$

This equation is true provided

$$\beta(\mathbf{k}_1) = \sum_{nn'} \frac{1}{2\pi i^{n+1}} Y_n(\hat{\mathbf{k}}_1) Q_{nn'}(\text{Re}, \text{Re}) \alpha_n^{(2)} \quad (39)$$

Equations 38 and 39 can be further manipulated to introduce the T-matrix of the buried scatterer. First we solve Eq. 38 for the expansion coefficients of the spherical wave basis functions by multiplying both sides by the inverse of the Q matrix to give

$$\begin{aligned} & \sum_n 4\pi i^n [Q^{-1}(\text{Out}, \text{Re})]_{mn} \int_0^{2\pi} d\phi_1 \int_{C_-} d\theta_1 \alpha(\mathbf{k}_1) Y_n(\hat{\mathbf{k}}_1) \sin \theta_1 \\ &= i \sum_{nn'} [Q^{-1}(\text{Out}, \text{Re})]_{mn} Q_{nn'}(\text{Out}, \text{Re}) \alpha_n^{(2)} \end{aligned}$$

Using the fact that

$$\sum_n [Q^{-1}(\text{Out}, \text{Re})]_{mn} Q_{nn'}(\text{Out}, \text{Re}) = \delta_{m,n'}$$

we have

$$\alpha_m^{(2)} = - \sum_n 4\pi i^{n+1} [Q^{-1}(\text{Out}, \text{Re})]_{mn} \int_0^{2\pi} d\phi_1' \int_{C_-} d\theta_1' \alpha(\mathbf{k}_1') Y_n(\hat{\mathbf{k}}_1') \sin \theta_1'$$

Substituting this into Eq. 37 and using the definition of the T-matrix of the scattering object  $T_{nm}(1)$

$$T_{nm}(1) = \sum Q_{nn'}(\text{Re}, \text{Re}) [Q^{-1}(\text{Out}, \text{Re})]_{n'm}$$

yields the relation between the upward propagating and downward propagating plane wave amplitudes in  $V_1$ .

$$\beta(\mathbf{k}_1) = 2 \sum_{nn'} i^{n+n'} Y_n(\hat{\mathbf{k}}_1) T_{nn'}(1) \int_0^{2\pi} d\phi'_1 \int_{C_-} d\theta'_1 \alpha(\mathbf{k}'_1) Y_{n'}(\hat{\mathbf{k}}'_1) \sin \theta'_1 \quad (40)$$

Equation 40 is the analog to the equation relating the incoming and scattered spherical wave amplitudes,  $\mathbf{f} = \mathbf{T}\mathbf{a}$ , that we derived above for acoustic scattering. Here, we have a more complicated equation since we are dealing with plane wave amplitudes and the spherical wave T-matrix of the scatterer. The spherical harmonics appearing in Eq. 40 and the integration are related to the transformations between the plane wave and spherical harmonic representations of the field.

In symbolic terms we can write the three remaining equations describing scattering from a buried object, Eqs. 36, 37, and 40, as

$$\begin{aligned} \mathbf{f} &= -i\mathbf{Q}_{f\alpha}\alpha - i\mathbf{Q}_{f\beta}\beta \\ \mathbf{a} &= i\mathbf{Q}_{a\alpha}\alpha + i\mathbf{Q}_{a\beta}\beta \\ \beta &= \mathbf{T}\alpha \end{aligned}$$

In these equations we have expressly identified each of the  $\mathbf{Q}$  functions as being different. Formally solving these equations yields

$$\mathbf{f} = -\mathbf{Q}_{f\beta}(\mathbf{Q}_{f\beta}^{-1}\mathbf{Q}_{f\alpha} + \mathbf{T})\mathbf{Q}_{a\alpha}^{-1}(\mathbf{I} + \mathbf{Q}_{a\beta}\mathbf{T}\mathbf{Q}_{a\alpha}^{-1})^{-1}\mathbf{a}$$

When the surface  $\sigma_0$  is flat, the  $\mathbf{Q}$  functions can be evaluated in terms of the reflection coefficient of the surface to give

$$\mathbf{f} = (R_{01} + \mathbf{T})(1 - R_{10}\mathbf{T})^{-1} \mathbf{a}$$

where:  $R_{01}$  is the reflection coefficient of a wave striking the interface from above and  $R_{10}$  is the reflection coefficient of a wave striking it from below. The total T matrix for the buried object is then

$$\mathbf{T}_{bur} = (R_{01} + \mathbf{T})(1 - R_{10}\mathbf{T})^{-1}$$

Noting that  $R_{10} = -R_{01}$ , this equation can be expanded in powers of the T matrix of the buried object to give the series

$$\mathbf{T}_{bur} = R_{01} + (1 - R_{01}R_{01})\mathbf{T} - (1 - R_{01}R_{01})\mathbf{T}R_{01}\mathbf{T} + \dots$$

Since  $1 - R_{01}R_{01} = T_{01}T_{10}$ , where  $T_{01}$  and  $T_{10}$  are the transmission coefficients of the interface, we have

$$\mathbf{T}_{bur} = R_{01} + T_{01}T_{10}\mathbf{T} + T_{01}T_{10}\mathbf{T}R_{10}\mathbf{T} + \dots$$

This expression has a simple physical interpretation. The T matrix of the buried object is made up of:

1. A reflection from the interface with no interaction with the buried scatterer
2. Transmission through the interface, interaction with the scatterer, and transmission back through the interface
3. Transmission through the interface, interaction with the scatterer, reflection from the underside of the interface, interaction with the scatterer, and transmission back through the interface
4. ...

#### H. Scattering in a Waveguide

For application to the analysis of scattering in shallow water, we need the theory of T-Matrix scattering in a waveguide. This is developed in Refs. 35-37. Our presentation here follows Ref. 37 which presents a compact theory for a homogenous waveguide that illustrates the basic physics without the complications of more general waveguide treated in Refs. 35 and 36.

We assume a horizontally stratified medium. The water column is bounded above by the sea surface and below by a layered seafloor terminated by a half

space. To develop the basic concepts, we first consider the case where both the source and scatterer are located in the same layer. After that, we will discuss the more realistic case where the source and scatterer are in different layers as would be the case for a source in the water and a scatterer buried in the seafloor. Cylindrical coordinates  $(\rho, z, \phi)$  with an origin inside the scatterer are used. The vector  $\vec{\rho}$  is the position in the x-y plane. A harmonic time dependence ( $e^{-i\omega t}$ ) is assumed.

## 7. Source and Scatterer in the Same Layer

The source and scatterer are bounded above by the plane  $z = a$  and below by the plane  $z = -b$ . The total acoustic field  $\Phi_{tot}$  is written as the sum of a source component  $\Phi_{src}$  and scattered component  $\Phi_{scat}$ .

$$\Phi_{tot} = \Phi_{src} + \Phi_{scat}$$

Each of the field components is expanded in a multiple-scattering series that takes into account the interaction with the medium above and below the layer containing the source and scatterer.

$$\Phi_{src} = \sum_{j=0}^{\infty} \sum_{i=1}^4 \Phi_{ji}^0$$

$$\Phi_{scat} = \sum_{j=0}^{\infty} \sum_{i=1}^4 \Phi_{ji}^s$$

The 4 terms in the sum over  $i$  are: the direct path ( $i=0$ ), the path reflecting once from the upper boundary ( $i=1$ ), the path reflecting once from the lower boundary ( $i=3$ ), and the path reflecting once from each boundary ( $i=4$ ). The direct path term is given by the free-field Green's function expanded in terms of upward and downward propagating plane waves

$$\Phi_{01}^0 = \frac{i}{4\pi} \int_0^{\infty} \frac{q dq}{h} J_0(q|\vec{\rho} - \vec{\rho}_s|) e^{\pm i h(z-z_s)}$$

where the field point is given by the cylindrical coordinates  $(\rho, z, \phi)$  and the source position is given by  $(\rho_s, z_s, \phi_s)$ . The positive sign in the exponent applies

when the field point is above the source position ( $z > z_s$ ) and the negative sign when the field point is below the source position ( $z < z_s$ ). The horizontal component of the wave vector  $k$  is  $q$  and the vertical component is  $h(q) = (k^2 - q^2)^{1/2}$ . For simplicity in keeping track of the signs in the exponents, we assume that  $z > z_s > 0$  in the following.

For the  $i=1$  term, we have plane waves propagating downward from the source ( $z=z_s$ ) to the boundary ( $z=-b$ ) followed by a reflection and propagation from  $z=-b$  to the field point.

$$\Phi_{02}^0 = \frac{i}{4\pi} \int_0^\infty \frac{q dq}{h} J_0(q|\rho - \rho_s|) \left[ e^{-ih(-b-z_s)} V e^{ih(z+b)} \right]$$

where  $V(q)$  is the plane wave reflection coefficient of the lower boundary, which will depend on  $q$  in the general case.

Similarly we have

$$\begin{aligned} \Phi_{03}^0 &= \frac{i}{4\pi} \int_0^\infty \frac{q dq}{h} J_0(q|\rho - \rho_s|) \left[ e^{ih(a-z_s)} U e^{-ih(z-a)} \right] \\ \Phi_{04}^0 &= \frac{i}{4\pi} \int_0^\infty \frac{q dq}{h} J_0(q|\rho - \rho_s|) \left[ e^{-ih(-b-z_s)} V e^{ih(a+b)} U e^{-ih(z-a)} \right] \end{aligned}$$

where  $U(q)$  is the plane wave reflection coefficient of the lower boundary of the layer. The  $i=4$  component is the multipath propagating downward at both the source and field point and having one interaction with each boundary. These four terms contain the direct path and three of the four multipaths having one interaction with each boundary. The fourth multipath (propagating upward from the source and arriving from below at the field point and interacting once with each boundary) is in the  $j=1$  part of the sum.

The  $j=1$  terms in the sum differ from the  $j=0$  terms by an additional scattering from both the upper and lower boundaries. This is accomplished by multiplying the  $j=0$  terms by a factor  $UV \exp(2ih(a+b))$ . Note that for the  $i=1$  term, the multiplication of the direct path by this factor produces the fourth multipath that was missing from the  $j=0$  sum.



The terms for any  $j$  are obtained from the  $j=0$  terms by multiplying by the factor  $[UV \exp(2ih(a+b))]^j$ . The resulting sum for the source field is

$$\Phi_{src} = \frac{i}{4\pi} \int_0^\infty \frac{q dq}{h} J_0(q|\rho - \rho_s|) \times \sum_{j=0}^4 \left( e^{ih(z-z_s)} + V e^{ih(z+z_s+2b)} + U e^{-ih(z+z_s-2a)} + UV e^{-ih(z-z_s-2(a+b))} \right) \times (UV e^{2ih(a+b)})^j \quad (41)$$

The geometric series can be summed to give

$$\Phi_{src} = \frac{i}{4\pi} \int_0^\infty \frac{q dq}{h} J_0(q|\rho - \rho_s|) \frac{1}{1 - UV e^{2ih(a+b)}} \left( e^{ih(z-a)} + U e^{-ih(z-a)} \right) \left( e^{-ih(z_s-a)} + V e^{2ih(a+b)} e^{ih(z_s-a)} \right)$$

The direct path contribution of the scatterer is the T-matrix of the scatterer. Using the spherical wave representation, this contribution is

$$\Phi_{01}^s = \sum_{pml} \sum_{p'm'l'} \psi_{pml}(\mathbf{r}) T_{pml, p'm'l'} C_{p'm'l'}$$

where:  $\psi_{pml}(\mathbf{r}) = h_l(kr) Y_{pml}(\theta, \phi)$  is an outgoing spherical wave,  $T$  is the transition matrix of the scatterer in spherical coordinates, and  $C_{pml}$  are the expansion coefficients of the total wave incident on the scatterer.

To use this in the cylindrical coordinate system of our waveguide we need the transformation between cylindrical and spherical wave functions. For the  $z$  axis of the scatterer parallel to the  $z$  axis of the coordinate system, this transformation is given by

$$\psi_{pml}(\mathbf{r}) = \left( \frac{\varepsilon_m}{2\pi} \right)^{1/2} \int_0^\infty \frac{q dq}{kh} B_{ml} \left( \pm \frac{h}{k} \right)^{-1} J_m(q\rho) e^{\pm i h z} \begin{cases} \cos m\phi, & p = \text{even} \\ \sin m\phi, & p = \text{odd} \end{cases}$$

where the plus sign is used for  $z > 0$  and the minus sign for  $z < 0$ . The  $B_{lm}$  functions convert the spherical functions into cylindrical functions and are given by

$$B_{ml}\left(\frac{h}{k}\right) = i^{l-m} \left( \frac{2l+1}{2} \frac{(l-m)!}{(l+m)!} \right)^{1/2} P_l^m\left(\frac{h}{k}\right) = B_{ml}\left(-\frac{h}{k}\right)^{-1}$$

where  $P_l^m$  are the associated Legendre functions.

Assuming that the field point is above the scatterer ( $z>0$ ) we use the plus sign in the transformation equation and obtain the following expression for the scattered field can be written as

$$\begin{aligned} \Phi_{scat} = & \sum_{pml} \left( \frac{\varepsilon_m}{2\pi} \right)^{1/2} \int_0^\infty \frac{q dq}{kh} J_m(q\rho) \begin{Bmatrix} \cos m\phi \\ \sin m\phi \end{Bmatrix} \\ & \times \sum_{j=0}^\infty \left[ e^{ihz} B_{ml}\left(\frac{h}{k}\right)^{-1} + V e^{ih(z+2b)} B_{ml}\left(-\frac{h}{k}\right)^{-1} + U e^{ih(2a-z)} B_{ml}\left(\frac{h}{k}\right)^{-1} + U V e^{-ih[z-2(a+b)]} B_{ml}\left(-\frac{h}{k}\right)^{-1} \right] \\ & \times (U V e^{2ih(a+b)})^j \sum_{p'm'l'} T_{pml, p'm'l'} c_{p'm'l'} \end{aligned} \quad (42)$$

The terms in the sum over  $j$  are : the scattered field propagating directly from the scatterer to the field point, the scattered field reflecting from the lower interface, the scattered field reflecting from the lower interface, and the scattered field reflecting once from each interface. As above, the term raised to the  $j^{th}$  power adds the additional multiples to the sum. The result is

$$\Phi_{scat} = -\frac{i}{k} \sum_{pml} A_{pml} \sum_{p'm'l'} T_{pml, p'm'l'} c_{p'm'l'} \quad (43)$$

where the vector  $\mathbf{A}$  is given by

$$\begin{aligned} A_{pml}(\mathbf{r}) = & i \left( \frac{\varepsilon_m}{2\pi} \right)^{1/2} \begin{Bmatrix} \cos m\phi \\ \sin m\phi \end{Bmatrix} \int_0^\infty \frac{q dq}{h} J_m(q\rho) \frac{1}{1 - U V e^{2ih(a+b)}} (e^{ih(z-a)} + U e^{-ih(z-a)}) \\ & \times \left[ B_{ml}\left(\frac{h}{k}\right)^{-1} e^{iha} + V e^{2ih(a+b)} B_{ml}\left(-\frac{h}{k}\right)^{-1} e^{-iha} \right] \end{aligned}$$

The next step is to determine the expansion coefficients of the total field incident on the scatterer. This is done using the "effective field" concept in which the

incident field is expressed as the source field and the scattered field with the direct scattering contribution removed, i. e.

$$\Phi_{incident} = \Phi_{src} + (\Phi_{scat} - \Phi_{01}^s)$$

Since none of the three terms above have singularities within the layer containing the source and scatterer, they can be expanded in terms of regular spherical wave functions. For this expansion, we have  $z < z_s$  since we are expanding about the origin of coordinates located within the scatterer. Note that this requires using the opposite sign for the exponential in the free-field Green's function than we have been using. For the incident wave we have the expansion used above,

$$\Phi_{incident} = \sum_{pml} c_{pml} \text{Re} \Psi_{pml}(\mathbf{r}) \quad (44)$$

For the source term we will convert Eq. 41 to spherical coordinates. The first step is to separate out the source and receiver parts of the Bessel function in Eq. 41 using

$$J_0(q|\rho - \rho_s|) = \sum_{m=0}^{\infty} \epsilon_m J_m(q\rho) J_m(q\rho_s) \cos m(\phi - \phi_s)$$

Next, expand the cosine and note that the two terms are equivalent to a sum over parity to get

$$J_0(q|\rho - \rho_s|) = 8\pi \sum_p \sum_{m=0}^{\infty} \frac{\epsilon_m}{8\pi} J_m(q\rho) J_m(q\rho_s) \begin{Bmatrix} \cos m(\phi) \cos m(\phi_s) \\ \sin m(\phi) \sin m(\phi_s) \end{Bmatrix}$$

This expression is nearly that of the regular cylindrical basis functions,

$$\text{Re} X_{pm}(\mathbf{r}) = \left( \frac{\epsilon_m}{8\pi} \right)^{1/2} J_m(q\rho) e^{ihz} \begin{Bmatrix} \cos m(\phi) \\ \sin m(\phi) \end{Bmatrix}$$

The missing exponential is contained in the multipath contributions to Eq. 41. Finally, using the transformation of the regular cylindrical basis functions to regular spherical basis functions,

$$\text{Re } X_{pm}(\mathbf{r}) = \sum_{l=0}^{\infty} B_{ml} \left( \frac{h}{k} \right) \text{Re } \Psi_{pml}$$

yields the expression for the source field

$$\Phi_{src} = \sum_{pml} A_{pml}(\mathbf{r}_s) \text{Re } \Psi_{pml}(\mathbf{r}) \quad (45)$$

Here, the vector  $\mathbf{A}$  is the same as that defined above for Eq. 42.

Using the same approach, the final term in the effective field equation can be obtained as

$$\Phi_{scat} - \Phi_{01}^s = i \sum_{pml, l'} \left( R_{l, l'}^m \sum_{p^* m^* l^*} T_{pml, p^* m^* l^*} c_{p^* m^* l^*} \right) \text{Re } \Psi_{pml}(\mathbf{r}) \quad (46)$$

where  $\mathbf{R}$  is the rescattering matrix given by

$$R_{l, l'}^m = -2i \int_0^{\infty} \frac{q dq}{hk} \frac{1}{1 - UV e^{2ih(a+b)}} \left[ UV B_{ml} \left( \frac{h}{k} \right) B_{ml'} \left( \frac{h}{k} \right)^{-1} e^{2ih(a+b)} + V B_{ml} \left( \frac{h}{k} \right) B_{ml'} \left( -\frac{h}{k} \right)^{-1} e^{2ihb} \right. \\ \left. + U B_{ml} \left( -\frac{h}{k} \right) B_{ml'} \left( \frac{h}{k} \right)^{-1} e^{2iha} + UV B_{ml} \left( -\frac{h}{k} \right) B_{ml'} \left( -\frac{h}{k} \right)^{-1} e^{2ih(a+b)} \right]$$

Combining Eqs. 44-46 in the equation for the effective field and equating the coefficients of the spherical basis functions gives us an equation for the expansion coefficients

$$c_{pml} = A_{pml}(\mathbf{r}_s) + i \sum_{l'} R_{l, l'}^m \sum_{p^* m^* l^*} T_{pml, p^* m^* l^*} c_{p^* m^* l^*}$$

In matrix notation, this equation is  $\mathbf{c} = \mathbf{A} + i\mathbf{R}\mathbf{T}\mathbf{c}$  which can be solved for the quantity  $\mathbf{T}\mathbf{c}$  that appears in Eq. 43,

$$\mathbf{T}\mathbf{c} = i(\mathbf{T}^{-1} + \mathbf{R})^{-1} \mathbf{A}$$

Using this in Eq. 43 yields the final result

$$\Phi_{total} = \Phi_{src} + \frac{1}{k} \mathbf{A}^T (\mathbf{T}^{-1} + \mathbf{R})^{-1} \mathbf{A}$$

This equation gives the total acoustic field as the sum of the source field (with boundary interactions) and the scattered field. Expanding the term containing the  $\mathbf{R}$  and  $\mathbf{T}$  matrices gives the series

$$i\mathbf{T} + \mathbf{T}\mathbf{R}\mathbf{T} + i\mathbf{T}\mathbf{R}\mathbf{T}\mathbf{R}\mathbf{T} + \dots$$

The contribution of the scatterer to the total field is the direct scattering term with corrections for the rescattering that occurs when the scattered field reflects from the boundaries and is again incident upon the scatterer.

## 8. Source and Scatterer in Different Layers

Figure 6 shows the geometry for source and scatterer in different layers. The source is in a layer bounded by  $z_1$  and  $z_2$ . The scatterer is in a layer bounded by  $z_3$  and  $z_4$ . The scatterer could be located in the seafloor or in the water column, depending on the location of  $z_3$ .

For this geometry, the Green's function contains the transmission coefficient of the acoustic field through the layers between the source and scatterer. In the following, we refer to the layer containing the source as layer 1 and the layer containing the scatterer as layer 2. We will use subscripts 1 and 2 to associate the quantities  $h$ ,  $k$ ,  $U$ , and  $V$  with the layer containing the source or the scatterer.

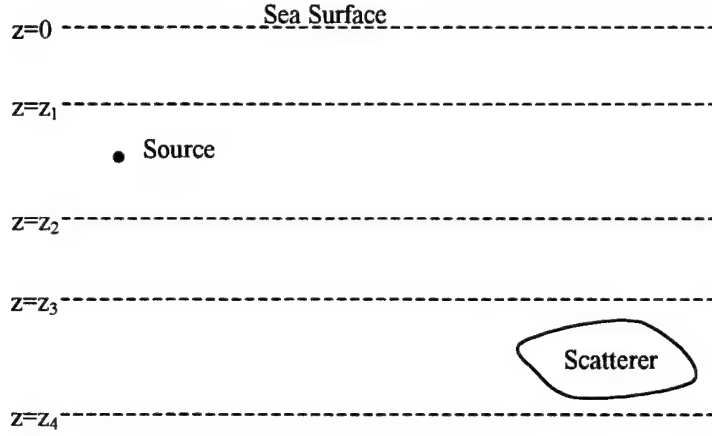


Figure 6. Geometry for source and scatterer in different layers

The Green's function for this cross-layer geometry is

$$G(\mathbf{r}_s, \mathbf{r}) = \frac{i}{4\pi} \int_0^\infty \frac{q dq}{h_1} J_0(q|\rho - \rho_s|) f_1(z_s) W f_2(z)$$

where:  $f_1(z_s)$  is the total acoustic field in layer 2 incident upon the interface at  $z_2$ ,  $f_2(z)$  is the total field at the point  $z$  in layer 2, and  $W$  is the total plane wave transmission coefficient through the layers between layer 1 and layer 2. After carrying out the multipath expansion of the fields in layers 1 and 2 as in the previous section, we find

$$f_1(z_s) = e^{-ih_1 z_s} \frac{(e^{ih_1 z_s} + U_1 e^{ih_1(2z_1 - z_s)})}{1 - U_1 V_1 e^{2ih_1(z_1 - z_2)}}$$

$$f_2(z) = e^{ih_2 z_3} \frac{(e^{-ih_2 z} + U_2 e^{-ih_2(2z_4 - z)})}{1 - U_2 V_2 e^{2ih_2(z_3 - z_4)}}$$

Inserting these into the Green's function yields the field produced by the source at a field point in layer 2,

$$\Phi_{src} = \frac{i}{4\pi} \int_0^\infty \frac{q dq}{h_1} J_0(q|\rho - \rho_s|) e^{-ih_1 z_s} \frac{(e^{ih_1 z_s} + U_1 e^{ih_1(2z_1 - z_s)})}{1 - U_1 V_1 e^{2ih_1(z_1 - z_2)}} W e^{ih_2 z_3} \frac{(e^{-ih_2 z} + U_2 e^{-ih_2(2z_4 - z)})}{1 - U_2 V_2 e^{2ih_2(z_3 - z_4)}}$$

The equation for  $A(\mathbf{r}_s)$  for the cross-layer geometry is

$$A_{pmi}(\mathbf{r}_s) = i \left( \frac{\varepsilon_m}{2\pi} \right)^{1/2} \left\{ \frac{\cos m\phi}{\sin m\phi} \right\} \int_0^\infty \frac{q dq}{h_1} J_m(q\rho_s) e^{-ih_1 z_s} \frac{(e^{ih_1 z_s} + U_1 e^{ih_1(2z_1 - z_s)})}{1 - U_1 V_1 e^{2ih_1(z_1 + z_2)}} W \\ \times e^{ih_2 z_3} \frac{\left[ B_{mi} \left( -\frac{h_2}{k_2} \right)^{-1} + V_2 e^{-2ih_2 z_4} B_{mi} \left( \frac{h_2}{k_2} \right)^{-1} \right]}{1 - U_2 V_2 e^{2ih_2(z_3 + z_4)}}$$

The rescattering matrix for the cross-layer geometry is obtained from that above by substituting  $z_3$  for  $a$ ,  $z_4$  for  $-b$ ,  $k_2$  for  $k$ ,  $U_2$  for  $U$ , and  $V_2$  for  $V$ .

### 9. Normal Mode Formulation

Moving the integration contour into the upper right quadrant recovers the normal mode formulation for the within-layer and cross-layer problems. The poles of the integrand occur at the zeros of the denominators. For the within-layer case the poles are defined by the equation  $(1 - UVe^{2ih(a+b)}) = 0$ . For the cross-layer case the defining equation is  $(1 - U_1 V_1 e^{2ih_1(z_1 + z_2)})(1 - U_2 V_2 e^{2ih_2(z_3 + z_4)}) = 0$ .

### I. Summary

The T-matrix approach is fully developed and contains all the tools needed for studying scattering from geological features buried in the seafloor. The theory for both acoustic and elastic wave scattering exists as well as extensions to multiple scattering and scattering in a waveguide.

## IV. P S COUPLING DUE TO GRADIENTS

Independently propagating shear and compressional waves can exist only when the acoustic properties of a material do not depend on position. When gradients exist, the two types of waves couple within the material as well as at interfaces between two different materials. Expanding in the inverse of the frequency, Richards<sup>42</sup> developed an asymptotic theory for the coupling of shear and compressional wave potentials and demonstrated decoupling at high frequencies. The unique and useful aspect of this theory is the use of second order, rather than fourth order, differential equations for the coupled potentials. Vidmar<sup>43</sup> extended this theory to a form valid for all frequencies that became the basis for estimates<sup>44</sup> that gradient-driven coupling is important only below about 10 Hz for deep sea sediments. Numerical studies<sup>45</sup> verified this estimate. Other

research<sup>46</sup> showed that gradient driven coupling generates shear waves when normal coupling at an interface does not take place, i. e., when the shear speed is zero at the interface.

Recent borehole tomography measurements<sup>47</sup> in shallow water indicate that volume inhomogeneities have gradients that are significantly larger (10 times, or more) than those found in deep ocean sediments. These enormously high gradients raise the possibility that gradient-driven PS conversion could be an important acoustical process at frequencies up to 1 kHz. A recent theory<sup>1</sup> of scattering from these inhomogeneities has been carried out but does not include shear wave coupling.

The remainder of this section reviews the theory of PS coupling as developed in Refs. 42 and 43.

#### A. Theory for Homogeneous Media

The description of motion in terms of potentials for a homogeneous layer illustrates the fundamental approach used for heterogeneous media. We begin with the equation of motion for the vector displacement  $\mathbf{u}$  for a material with density  $\rho$  and Lamé parameters  $\lambda$ , and  $\mu$

$$\rho\omega^2\mathbf{u} = -(\lambda + 2\mu)\nabla\nabla\cdot\mathbf{u} + \mu\nabla\times\nabla\times\mathbf{u} \quad (47)$$

and the decomposition of the displacement into compressional and shear potentials as

$$\mathbf{u} = \nabla\Phi + \nabla\times\tilde{\Psi} \quad (48)$$

The usual procedure is to substitute Eq. 48 into Eq. 47 (assuming that  $\nabla\cdot\tilde{\Psi} = 0$ ) yielding a third order differential equation. Further manipulation results in two decoupled fourth order differential equations for the compressional and shear wave potentials.

$$\begin{aligned} \nabla^2 \left\{ \nabla^2 \Phi + \frac{\omega^2}{c_p^2} \Phi \right\} &= 0 \\ \nabla^2 \left\{ \nabla^2 \tilde{\Psi} + \frac{\omega^2}{c_s^2} \tilde{\Psi} \right\} &= 0 \end{aligned}$$



where we have used the definitions of the shear speed  $c_s^2 = \mu/\rho$  and the compressional speed  $c_p^2 = (\lambda + 2\mu)/\rho$ .

Upon assuming that the quantities in brackets are zero, we have the usual second order differential equations for the potentials. When applied to heterogeneous media, this approach yields coupled fourth order differential equations.<sup>48</sup>

Another approach is to note that Eq. 47 already has the form of Eq. 48 and to then define the potentials directly from Eq. 47 as

$$\Phi = -\frac{\omega^2}{c_p^2} \nabla \cdot \mathbf{u}$$

$$\tilde{\Psi} = -\frac{\omega^2}{c_s^2} \nabla \times \mathbf{u}$$

It follows from Eq. 47 that

$$\nabla^2 \Phi + \frac{\omega^2}{c_p^2} \Phi = 0$$

$$\nabla^2 \tilde{\Psi} + \frac{\omega^2}{c_s^2} \tilde{\Psi} = 0$$

$$\nabla \cdot \tilde{\Psi} = 0$$

This approach avoids using fourth order differential equations and, when generalized to heterogeneous media, it produces coupled second order differential equations.

## B. Theory for Heterogeneous Media

We begin with the equation of motion for a heterogeneous solid in Cartesian coordinates<sup>49</sup>. For simplicity, we consider wave motion in the x-z plane in a material with gradients in the z direction only. The time dependence is  $e^{-i\omega t}$ . The dependence on x is given by  $e^{i\delta x}$  which follows from spatial invariance along the x axis.

## 1. Weakly Coupled Potentials

The resulting equation of motion for a harmonic wave is

$$\rho\omega^2\mathbf{u} = -(\lambda + 2\mu)\nabla\nabla\cdot\mathbf{u} + \mu\nabla\times\nabla\times\mathbf{u} - \lambda'\hat{\mathbf{z}}\nabla\cdot\mathbf{u} - \mu'\left(\hat{\mathbf{z}}\times\nabla\times\mathbf{u} + 2\frac{\partial\mathbf{u}}{\partial z}\right) \quad (49)$$

where  $\hat{\mathbf{z}}$  is a unit vector in the direction of the positive  $z$  axis and the prime indicates a derivative with respect to  $z$ .

We next assume that the displacement can be written in terms of potentials with some additional functions that will allow us to recover Eq. 49.

$$\mathbf{u} = \frac{1}{f_1}\nabla\Phi + \frac{1}{f_2}\nabla\times\tilde{\Psi} - \mathbf{s} \quad (50)$$

For motion in the  $x$ - $z$  plane, the vector potential is given by  $\tilde{\Psi}(x, z) = \hat{\mathbf{y}}\Psi(x, z)$  where  $\hat{\mathbf{y}}$  is a unit vector along the positive  $y$  axis. As in the homogeneous case, we define the potentials in terms of the displacement vector, but with some additional (as yet unknown) functions in the definition.

$$\Phi = \alpha\nabla\cdot(f_2\mathbf{u}) \quad (51)$$

$$\tilde{\Psi} = \beta\nabla\times(f_1\mathbf{u})$$

The functions  $f_1$ ,  $f_2$ ,  $\alpha$ , and  $\beta$  depend on  $z$  alone. They will allow Eq. 50 to duplicate the first and second derivative terms in Eq. 49. The vector  $\mathbf{s}$  contains the remaining terms in Eq. 47 that are linear in the components of  $\mathbf{u}$ . We proceed by calculating the quantity

$$\mathbf{u}^* = \frac{1}{f_1}\nabla\Phi + \frac{1}{f_2}\nabla\times\tilde{\Psi}$$

and comparing the resulting expression with Eq. 49.

The two terms of  $\mathbf{u}^*$  are

$$\frac{1}{f_1} \nabla \Phi = \alpha \frac{f_2}{f_1} \nabla (\nabla \cdot \mathbf{u}) + \hat{\mathbf{z}} (\alpha f_2)' \nabla \cdot \mathbf{u} + \frac{\alpha f_2'}{f_1} \left( \hat{\mathbf{z}} \times (\nabla \times \mathbf{u}) + \frac{\partial \mathbf{u}}{\partial z} \right) + \frac{(\alpha f_2')'}{f_1} \hat{\mathbf{z}} (\hat{\mathbf{z}} \cdot \mathbf{u}) \text{ and}$$

$$\frac{1}{f_2} \nabla \times \bar{\Psi} = \frac{\beta f_1}{f_2} \nabla \times (\nabla \times \mathbf{u}) + \frac{(\beta f_1)'}{f_2} \hat{\mathbf{z}} \times (\nabla \times \mathbf{u}) + \frac{\beta f_1'}{f_2} \left[ \hat{\mathbf{z}} (\nabla \cdot \mathbf{u}) - \frac{\partial \mathbf{u}}{\partial z} \right] + \frac{(\beta f_1')}{f_2} \hat{\mathbf{z}} \times (\hat{\mathbf{z}} \times \mathbf{u})$$

Comparing the terms containing the second derivative of  $\mathbf{u}$  in  $\mathbf{u}^*$  with Eq. 49 provides the following two equations.

$$\alpha \frac{f_2}{f_1} = -\frac{(\lambda + 2\mu)}{\rho \omega^2} \quad (52)$$

$$\beta \frac{f_1}{f_2} = \frac{\mu}{\rho \omega^2}$$

The first derivative terms provide the following three equations.

$$\frac{(\alpha f_2)'}{f_1} + \frac{\beta f_1'}{f_2} = -\frac{\lambda'}{\rho \omega^2}$$

$$\frac{\alpha f_2'}{f_1} + \frac{(\beta f_1)'}{f_2} = -\frac{\mu'}{\rho \omega^2} \quad (53)$$

$$\frac{\alpha f_2'}{f_1} - \frac{\beta g_1'}{f_2} = -2 \frac{\mu'}{\rho \omega^2}$$

Defining  $g_1 = f_1'/f_1$  and  $g_2 = f_2'/f_2$ , solving for  $\alpha$  and  $\beta$  in Eq. 52, and substituting into the first two equations of Eq. 53 yields the following.

$$g_1 = \frac{\lambda + 2\mu}{\lambda + \mu} \left( \frac{\rho'}{\rho} - \frac{2\mu'}{\lambda + 2\mu} \right) \quad (53)$$

$$g_2 = \frac{\mu}{\lambda + \mu} \left( \frac{2\mu'}{\mu} - \frac{\rho'}{\rho} \right)$$

We note that  $g_1 + g_2 = \rho'/\rho$  and that  $g_1$  and  $g_2$  depend only on the properties of the material. Substituting  $\alpha$ ,  $\beta$ ,  $g_1$ , and  $g_2$  into the third equation of Eq. 53 produces an identity. Once we know  $g_i$  in terms of the material parameters, it is easy to calculate  $f_i$ . From the definition of  $g_i$  it is the depth derivative of  $\ln(f_i)$ . Integrating over depth from the top of the sediment, and assuming a value of one at the sediment surface, we have

$$f_i(z) = e^{\int_0^z d\zeta g_i(\zeta)}$$

We next recover Eq. 49 by defining  $\mathbf{s}$  as containing the terms in  $\mathbf{u}^*$  which are linear in  $\mathbf{u}$ .

$$\mathbf{s} = \frac{(\alpha f_2')}{f_1} \hat{\mathbf{z}}(\hat{\mathbf{z}} \cdot \mathbf{u}) + \frac{(\beta f_1')}{f_1} \hat{\mathbf{z}} \times (\hat{\mathbf{z}} \times \mathbf{u}) \quad (55)$$

Manipulating the coefficients in Eq. 55 and substituting into Eq. 50 gives us

$$\mathbf{u} = \frac{1}{f_1} \nabla \Phi + \frac{1}{f_2} \nabla \times \bar{\Psi} + \frac{\omega_1^2}{\omega^2} \hat{\mathbf{x}} u_x + \frac{\omega_2^2}{\omega^2} \hat{\mathbf{z}} u_z \quad (56)$$

where

$$\begin{aligned} \omega_1^2 &= \frac{1}{\rho} (\mu' g_1 + \mu g_1' + \mu g_1 g_1') \\ \omega_2^2 &= \frac{1}{\rho} [(\lambda + 2\mu)' g_2 + (\lambda + 2\mu) g_2' + (\lambda + 2\mu) g_2 g_2'] \end{aligned} \quad (57)$$

The differential equation for  $\Phi$  is obtained by multiplying Eq. 56 by  $f_2$ , taking the divergence of the result, and multiplying by  $\alpha$  to produce  $\Phi$  as defined in Eq. 51. Multiplying Eq. 56 by  $f_1$ , taking the curl, and multiplying by  $\beta$  produces the differential equation for  $\Psi$ . The results are

$$\begin{aligned}\nabla^2 \Phi + (g_2 - g_1)\Phi' + D_1 \left( \frac{\rho \omega^2}{\lambda + 2\mu} \right) \Phi &= f_1 [D_2' + g_2(D_2 - D_1)]u_z + f_1(D_2 - D_1)u_z' \\ \nabla^2 \Psi + (g_1 - g_2)\Psi' + D_2 \left( \frac{\rho \omega^2}{\mu} \right) \Psi &= f_2 [-D_1' + g_1(D_2 - D_1)]u_x + f_2(D_2 - D_1)u_x'\end{aligned}\quad (58)$$

In Eq. 58 we have defined two auxiliary functions  $D_1$  and  $D_2$  as

$$\begin{aligned}D_1 &= 1 - \frac{\omega_1^2}{\omega^2} \\ D_2 &= 1 - \frac{\omega_2^2}{\omega^2}\end{aligned}\quad (59)$$

Equation 58 shows the high frequency decoupling of the potentials  $\Phi$  and  $\Psi$ . From Eq. 59, the terms involving  $D_1 - D_2$  and the derivatives of  $D_1$  and  $D_2$  are proportional to  $1/\omega^2$ . Using Eq. 56 to substitute for the components of the displacement in Eq. 58 produces two terms proportional to  $1/\omega^2$  involving both potentials (hence, the coupling between them) and two additional terms proportional to  $1/\omega^4$  involving the components of the displacement. Continuing the process generates a series involving  $1/\omega^2$  to higher powers multiplying increasingly high derivatives of the potentials. To show decoupling, one argues that for sufficiently high frequencies the right side of Eq. 58 is negligible compared to the left side. Hence, the potentials are essentially decoupled at high frequencies. While this argument is true, it is not clear just how high in frequency one must go to achieve decoupling in view of the increasingly higher order derivatives of the potentials appearing on the right side of Eq. 58. We address this difficulty below and derive a quantitative definition of the decoupling frequency. Decoupling also occurs for special materials for which  $D_1' = D_2' = 0$  and  $D_1 = D_2$ .

## 2. Exact Coupled Potentials

We follow Ref. 43 to derive second order differential equations for  $\Phi$  and  $\Psi$  that are exact, i. e., they do not contain the components of the displacement. We start out by writing Eq. 56 in component form and combine terms to obtain

$$\begin{aligned}D_1 u_x &= \left[ \frac{1}{f_1} (\nabla \Phi)_x + \frac{1}{f_2} (\nabla \times \tilde{\Psi})_x \right] \\ D_2 u_z &= \left[ \frac{1}{f_1} (\nabla \Phi)_z + \frac{1}{f_2} (\nabla \times \tilde{\Psi})_z \right]\end{aligned}\quad (60)$$

We now write Eq. 60 in vector form by defining a coupling tensor  $\mathbf{C}$  and its inverse as

$$\mathbf{C} = \begin{pmatrix} D_1 \hat{\mathbf{x}}\hat{\mathbf{x}} & 0 \\ 0 & D_2 \hat{\mathbf{z}}\hat{\mathbf{z}} \end{pmatrix} \quad (60)$$

$$\mathbf{C}^{-1} = \begin{pmatrix} \frac{1}{D_1} \hat{\mathbf{x}}\hat{\mathbf{x}} & 0 \\ 0 & \frac{1}{D_2} \hat{\mathbf{z}}\hat{\mathbf{z}} \end{pmatrix}$$

Substituting into Eq. 58 gives an equation for the displacement in terms of the potentials without extra displacement components on the right side.

$$\mathbf{u} = \mathbf{C}^{-1} \cdot \left( \frac{1}{f_1} \nabla \Phi + \frac{1}{f_2} \nabla \times \bar{\Psi} \right) \quad (62)$$

The next step is to use Eq. 62 and Eq. 51 to again derive the differential equations for the potentials. As in the previous section, we multiply Eq. 62 by  $f_2$ , take the divergence, and multiply by  $\alpha$  to produce the differential equation for  $\Phi$ . Multiplying Eq. 62 by  $f_1$ , taking the curl, and multiplying by  $\beta$  produces the differential equation for  $\Psi$ . Recalling that the  $x$  dependence of the potentials is through  $e^{i\delta x}$ , the result is

$$\Phi'' + \left( g_2 - g_1 - \frac{D_2'}{D_2} \right) \Phi' + \frac{D_2}{D_1} \left( D_1 \frac{\omega^2}{c_p^2} - \delta^2 \right) \Phi = i\delta \frac{f_1}{f_2} \left[ \frac{D_2'}{D_2} \Psi + \left( \frac{D_2}{D_1} - 1 \right) \Psi' \right] \quad (63)$$

$$\Psi'' + \left( g_1 - g_2 - \frac{D_1'}{D_1} \right) \Psi' + \frac{D_1}{D_2} \left( D_2 \frac{\omega^2}{c_s^2} - \delta^2 \right) \Psi = -i\delta \frac{f_2}{f_1} \left[ \frac{D_1'}{D_1} \Phi + \left( \frac{D_1}{D_2} - 1 \right) \Phi' \right]$$

The terms on the right side of Eq. 63 provide the coupling between the potentials without reference to components of the displacement.

### 3. Displacement and Stress for Exact Coupled Potentials

We need to know how to express the components of the displacement vector and the stress tensor in order to carry out numerical computations. The results for the displacement follow directly from Eq. 62.

$$u_x = \frac{1}{D_1} \left( \frac{i\delta}{f_1} \Phi - \frac{1}{f_2} \Psi' \right)$$

$$u_z = \frac{1}{D_2} \left( \frac{1}{f_1} \Phi' + \frac{i\delta}{f_2} \Psi \right)$$

The expressions for the stress tensor are also straightforward, but tedious, to derive. The results are

$$T_{zz} = -\rho \left( \omega^2 - \frac{2c_s^2 \delta^2}{D_1} \right) \frac{\Phi}{f_1} - \rho \frac{g_2 c_p^2}{D_2} \frac{\Phi'}{f_1} - \rho \frac{g_2 c_p^2 i \delta}{D_2} \frac{\Psi}{f_2} + \rho \frac{2c_s^2 i \delta}{D_1} \frac{\Psi'}{f_2}$$

$$T_{xz} = \rho \left( \omega^2 - \frac{2c_s^2 \delta^2}{D_2} \right) \frac{\Psi}{f_2} + \rho \frac{g_1 c_s^2}{D_1} \frac{\Psi'}{f_2} - \rho \frac{g_1 c_s^2 i \delta}{D_1} \frac{\Phi}{f_1} + \rho \frac{2c_s^2 i \delta}{D_2} \frac{\Phi'}{f_1}$$

### 4. Decoupling of Exact Potentials

Decoupling of  $\Phi$  and  $\Psi$  occurs under two conditions. First, there is decoupling at high frequencies. Because coupling terms are proportional to the derivatives of  $D_1$  and  $D_2$  or to  $D_1 - D_2$  decoupling occurs at high frequencies in agreement with Ref. 42. The second kind of decoupling occurs for particular media for which  $D_1' = D_2' = 0$  and  $D_1 = D_2$ . This is the case for the material found in Ref. 50 for which  $\mu = \mu_1(1+bz)^2$ ,  $\lambda = \lambda_1(1+bz)^2$ ,  $\lambda_1 = \mu_1$ , and  $\rho = \rho_1$ . Direct substitution into Eqs. 57 and 59 yields  $\omega_1^2 = \omega_2^2 = -6\mu_1 b^2$  and verifies decoupling at all frequencies. Note that in evaluating Eq. 57 we do not need to know  $f_1$  and  $f_2$  but only  $g_1$  and  $g_2$ , which are defined in terms of material parameters.

### 5. Resonance Frequencies

Equation 63 has an interesting feature. There is a potential resonance in the system at the frequencies  $\omega_1$  and  $\omega_2$  for which the denominators in several terms of Eq. 63 can be zero. The significance of this resonance has not been fully

explored. Here, we examine the resonant frequencies as a function of the gradients of seafloor parameters.

The first step is to develop expressions for the resonant frequencies based on density, shear velocity, compressional velocity. Equation 57 gives the resonant frequencies in terms of  $g_1$ ,  $g_2$ , the density and the depth derivative of the Lamé parameters. Our goal here is to develop an expression that involves more readily obtainable quantities such as density, shear velocity and compressional velocity. We start by introducing the shear and compressional velocities into Eq. 57 and eliminating the derivatives of the Lamé parameters using the following relations obtained from the derivative of the definition of the shear and compressional velocities

$$\frac{\mu'}{\mu} = \frac{\rho'}{\rho} + 2 \frac{c_s'}{c_s}$$

$$\frac{(\lambda + 2\mu)'}{\lambda + 2\mu} = \frac{\rho'}{\rho} + 2 \frac{c_p'}{c_p}$$

The resulting resonant frequencies are

$$\omega_1^2 = c_s^2 \left[ \left( \frac{\rho'}{\rho} + 2 \frac{c_s'}{c_s} + g_1 \right) g_1 + g_1' \right]$$

$$\omega_2^2 = c_p^2 \left[ \left( \frac{\rho'}{\rho} + 2 \frac{c_p'}{c_p} + g_2 \right) g_2 + g_2' \right]$$

$g_1$ , and  $g_2$  and their derivatives are given by

$$g_1 = \frac{1}{c_p^2 - c_s^2} \left[ (c_p^2 - 2c_s^2) \frac{\rho'}{\rho} - 4c_s^2 \frac{c_s'}{c_s} \right]$$

$$g_2 = \frac{c_s^2}{c_p^2 - c_s^2} \left[ \frac{\rho'}{\rho} + 4 \frac{c_s'}{c_s} \right]$$

and



$$\begin{aligned}
g'_1 &= \frac{1}{c_p^2 - c_s^2} \left\{ (c_p^2 - 2c_s^2) \left[ \frac{\rho''}{\rho} - \left( \frac{\rho'}{\rho} \right)^2 \right] - 4c_s^2 \frac{c_s''}{c_s} \right. \\
&\quad \left. - \frac{2c_s^2}{c_p^2 - c_s^2} \left[ 2(c_p^2 + c_s^2) \left( \frac{c'_s}{c_s} \right)^2 + c_p^2 \left( \frac{\rho' c'_s}{\rho c_s} - \frac{\rho' c'_p}{\rho c_p} - \frac{c'_s c'_p}{c_s c_p} \right) \right] \right\} \\
g'_2 &= \frac{c_s^2}{c_p^2 - c_s^2} \left\{ \frac{\rho''}{\rho} - \left( \frac{\rho'}{\rho} \right)^2 + 4 \frac{c_s''}{c_s} \right. \\
&\quad \left. + \frac{2}{c_p^2 - c_s^2} \left[ 2(c_p^2 + c_s^2) \left( \frac{c'_s}{c_s} \right)^2 + c_p^2 \left( \frac{\rho' c'_s}{\rho c_s} - \frac{\rho' c'_p}{\rho c_p} - \frac{c'_s c'_p}{c_s c_p} \right) \right] \right\}
\end{aligned}$$

#### a) Resonance Frequencies for Typical Sediments

In this section we estimate the resonance frequencies for typical sediments. First, we will use typical values for gradients to identify the driving terms in the expressions for  $g_1$ ,  $g_2$ , and their derivatives. Typical parameters for near surface sediments<sup>51</sup> are given in Table 2.

	Clay	Medium Sand
<b>Density</b>	1.40 g/cc	2.00 g/cc
<b>Compressional Velocity</b>	1490 m/s	1620 m/s
<b>Shear Velocity</b>	50 m/s	150 m/s

Table 2. Typical values of surficial sediment parameters.

Using the fact that  $c_s^2/c_p^2 \approx 1 \times 10^{-3}$  for clay and assuming that second derivatives are negligible, the expressions for  $g_1$ ,  $g_2$ , and their derivatives are approximately given by

$$\begin{aligned}
g_1 &\approx \frac{\rho'}{\rho} - 4 \frac{c_s^2}{c_p^2} \frac{c'_s}{c_s} \\
g_2 &\approx \frac{c_s^2}{c_p^2} \left( \frac{\rho'}{\rho} + 4 \frac{c'_s}{c_s} \right) \\
g'_1 &\approx - \left( \frac{\rho'}{\rho} \right)^2 - 2 \frac{c_s^2}{c_p^2} \left[ 2 \left( \frac{c'_s}{c_s} \right)^2 + \frac{\rho' c'_s}{\rho c_s} - \frac{\rho' c'_p}{\rho c_p} - \frac{c'_s c'_p}{c_s c_p} \right] \\
g'_2 &\approx \frac{c_s^2}{c_p^2} \left\{ - \left( \frac{\rho'}{\rho} \right)^2 + 2 \left[ 2 \left( \frac{c'_s}{c_s} \right)^2 + \frac{\rho' c'_s}{\rho c_s} - \frac{\rho' c'_p}{\rho c_p} - \frac{c'_s c'_p}{c_s c_p} \right] \right\}
\end{aligned}$$

We next identify the dominant terms involving the parameter gradients. For deep ocean sediments (clay), typical gradients are:  $\rho' = 1.2 \times 10^{-3} \text{ g/cc/m}$ ,  $c_p' = 1.5 / \text{s}$ , and  $c_s' = 4.0 / \text{s}$ . The values of the ratios of the parameters to their derivatives are approximately  $\rho'/\rho \approx 1 \times 10^{-3} / \text{m}$ ,  $c_p'/c_p \approx 1 \times 10^{-3} / \text{m}$ , and  $c_s'/c_s \approx 1 \times 10^{-1} / \text{m}$ . The relative gradients of density and compressional velocity are comparable while the relative gradient of shear speed is about two orders of magnitude larger.

Keeping only the most significant terms in the expressions for the resonance frequencies, we obtain

$$\omega_1^2 \approx 2c_s^2 \frac{\rho' c_s'}{\rho c_x} \text{ and } \omega_2^2 = 4c_s^2 \left( \frac{c_s'}{c_x} \right)^2$$

Substituting numerical values we estimate the resonant frequencies to be

$$f_1 \approx \frac{\omega_1}{2\pi} \approx .07 \text{ Hz and } \frac{\omega_2}{2\pi} \approx 1.6 \text{ Hz}$$

Thus, gradient driven coupling of compressional and shear waves is negligible for deep sea sediments for frequencies above about 10 Hz. Since parameter values for shallow water sediments do not change by orders of magnitude, the same conclusion is true for shallow water sediments.

#### b) Resonance Frequencies for Volume Inhomogeneities.

As discussed at the beginning of this section, there is evidence<sup>47</sup> that volume inhomogeneities in shallow water sediments have parameter gradients that are significantly larger (10 times, or more) than the large scale gradients. In this section, we present estimates of the resonance frequencies associated with these gradients. To estimate gradients we assumed a transition from a clay to a sand sediment over distances from 1 cm to 20 m.

Figure 7 shows that the resonance frequency can be quite large for a thin transition layer. Frequencies above 1 kHz occur for transition layers of 1-5 cm, not an unreasonable thickness for volume inhomogeneities. For transition layers about 10 m thick, the resonance frequencies are on the order of 1 Hz, the value estimated for deep water sediment types.

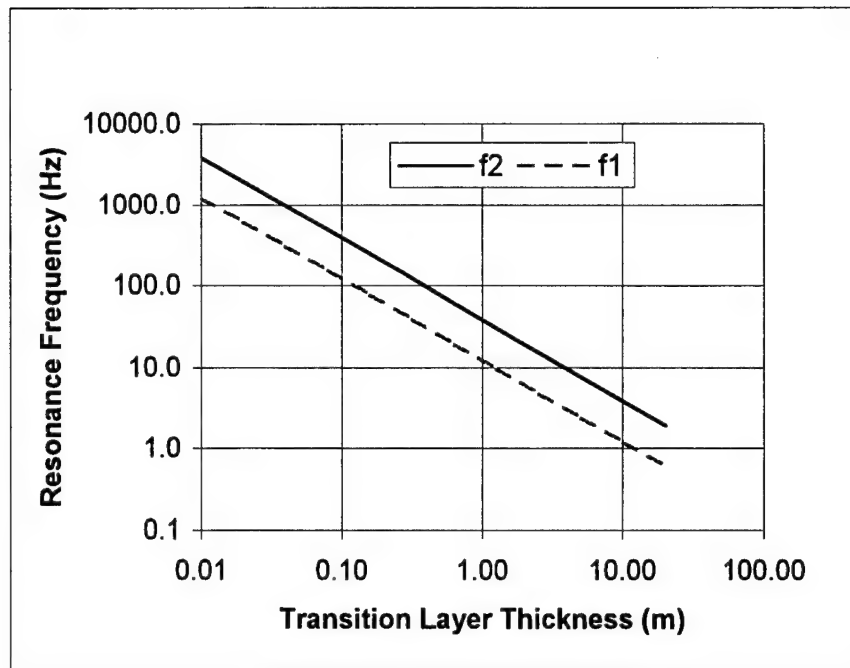


Figure 7. Dependence of resonance frequency on transition layer thickness.

### C. Summary

We reviewed the theoretical treatment of gradient driven coupling of compressional and shear waves. The theory of a homogeneous layer showed the basic approach for developing second order, rather than fourth order, differential equations for the coupled potentials. The basic concept introduced was that of defining the potentials in terms of the displacements. Applying this concept to a depth dependent layer yielded two differential equations for weakly coupled potentials, for which the coupling is proportional to the inverse of the square of the frequency. The potentials reduce to the ordinary shear and compressional potentials for a homogeneous media. The two potentials are coupled by terms in the displacements. A refinement of the theory, using tensor scale factors, produced exact coupled differential equations with the coupling terms related to the potentials and their derivatives.

The differential equations for the exact coupled potentials demonstrate decoupling at high frequencies and at all frequencies for media with specific properties. Decoupling at high frequencies occurs when the frequency is large compared to two frequencies whose values depend on the material parameters and their gradients. These frequencies are called "resonance frequencies" since they appear in the denominators of terms in the differential equations. Should the frequency be equal to one of the resonance frequencies, the denominators

vanish. The significance of these resonance effects has not been examined. For typical deep sea sediments the resonance frequencies are around 1 Hz. They can be on the order of 1000 Hz for the large gradients thought to occur for volume inhomogeneities in shallow water sediments.

## V. RECOMMENDATIONS

Our investigation of T-Matrix theory and the theory of gradient driven coupling of shear and compressional waves finds that both hold great promise for developing an understanding of scattering from the subbottom in shallow water areas.

Below we give our recommendations for further work.

### A. T-Matrix

The T-matrix approach to scattering is well developed and contains almost all the tools needed to address some of the issues dealing with the time spread induced by scattering from the seafloor. One such issue is the role of scattering from sedimentary layers with finite lateral extent. Scattering from the edges of layers is one possible mechanism for producing backscatter from regions with a smooth sediment surface. Another is the problem of predicting the attenuation parameter of sedimentary materials for Navy databases. At present the attenuation is a "total energy" attenuation which includes effects of scattering as well as intrinsic attenuation. Understanding these issues would provide the basis for improvements to the geoacoustic databases used by the Navy to predict the performance of sonar systems.

The approach we recommend would be to first develop numerical models of the T-matrix of several canonical objects that would serve as entries in a catalog of scatterers. The objects would include: (1) nearly spherical layered objects that would approximate a density or velocity inhomogeneity, (2) scatterers approximating the shape of gas trapped in sediments (spherical to disk shaped), (3) pancake shaped (oblate spheroid), fluid, object with a thickness and lateral extent typical of sedimentary layering, and (4) objects approximating the shape of other buried objects such as rocks and shells. The numerical models must be broadband so the impulse response of the scatterer can be obtained as an inverse Fourier transform. Once the T-matrix is available, the methods summarized above can be applied to study scattering from single objects buried in a background sediment. Next, scattering from several objects in a typical geometry would be studied to determine the importance of multiple scattering, edge effects, and orientation relative to the horizontal. Scattering from several realizations of the layering would be carried out to understand the variability of scattering and time spread. Finally, scattering in a waveguide would be

examined using simplified models based on the earlier work with the goal of determining the importance of scattering in relation to attenuation and other parameters.

## B. Gradient Driven Coupling

The theory for gradient driven coupling of compressional and shear waves is well developed with two exceptions. First, a stochastic theory does not exist. Such a theory is needed to explore the role of gradient driven coupling for volume inhomogeneities. Second, the significance of the resonance frequencies described above has not been explored. If the resonance leads to instability in the system, it might be related to the onset of seismic activity. For the high gradients estimated for volume inhomogeneities in shallow water, the resonance could be an important loss process converting compressional energy to shear energy with greater efficiency than coupling at an interface between two layers. We recommend further research to address these issues.

A fully developed theory of gradient driven coupling would provide the basis for determining the importance of coupling to shear waves through scattering from volume inhomogeneities. This is an important issue to resolve since it has implications for the content of Navy geoacoustic databases and the complexity of Navy performance prediction models. If shear wave coupling is important, new propagation models will be needed that will typically require an order of magnitude more computational resources than current models. If shear coupling is not important, simplified models and databases can be used.

## REFERENCES

1. T. Yamamoto, "Acoustic scattering in the ocean from velocity and density fluctuations in the sediments," *J. Acoust. Soc. Am.* **99**, 866-879 (1996).
2. A. P. Lyons and A. Anderson, "Acoustic scattering from the seafloor: Modeling and data comparison," *J. Acoust. Soc. Am.* **95**, 2441-2451 (1995).
3. T. Yamamoto, "Velocity variabilities and other physical properties of marine sediments measured by crosswell acoustic tomography," *J. Acoust. Soc. Am.* **98**, 2235-2248 (1995).
4. J. A. Goff and T. H. Jordan, "Stochastic modeling of seafloor morphology: A parameterized Gaussian model," *Geophys. Res. Lett.* **16**, 45-48 (1989).
5. T. H. Orsi, Jr., "Computed tomography of macrostructure and physical property variability of seafloor sediments," Ph.D. dissertation, Texas A&M University, College Station, Texas, August 1994.
6. P. C. Waterman, "New formulation of acoustic scattering," *J. Acoust. Soc. Am.* **45**, 1417-1429 (1966).
7. V. V. Varadan, A. Lakhtakia, and V. K. Varadan, "Comments on recent criticism of the T-matrix method," *J. Acoust. Soc. Am.* **84**, 2280-2284 (1988).
8. *Acoustic, Electromagnetic and Elastic Wave Scattering—Focus on the T-Matrix Approach*, edited by V. K. Varadan and V. V. Varadan (Pergamon Press, New York, 1980).
9. *Field Representations and Introduction to Scattering*, edited by V. V. Varadan, A. Lakhtakia, and V. K. Varadan, (North-Holland, New York, 1991).
10. M. F. Werby and N. A. Sidorovskaia, "Modern developments in the theory and application of classical scattering," in preparation, Naval Research Laboratory, Stennis Space Center, Mississippi (1996).
11. P. C. Waterman, "Matrix theory of elastic wave scattering," *J. Acoust. Soc. Am.* **60**, 567-580 (1976).
12. P. C. Waterman, "Matrix theory of elastic wave scattering. II. A new conservation law," *J. Acoust. Soc. Am.* **63**, 1320-1325 (1978).
13. Y. Pao and V. Varatharajulu, "Huygens' principle, radiation conditions, and integral formulas for the scattering of elastic waves," *J. Acoust. Soc. Am.* **59**, 1361-1371 (1976).
14. V. Varatharajulu and Y. Pao, "Scattering matrix for elastic waves. I. Theory," *J. Acoust. Soc. Am.* **60**, 556-567 (1976).
15. V. Varatharajulu, "Reciprocity relations and forward amplitude theorems for elastic waves," *J. Math. Phys.* **18**, 537-543 (1977).
16. Y. Pao, "Betti's identity and transition matrix for elastic waves," *J. Acoust. Soc. Am.* **64**, 302-310 (1978).
17. P. C. Waterman, "Matrix methods in potential theory and electromagnetic scattering," *J. Appl. Phys.* **50**, 4550-4566 (1979).
18. B. Peterson, V. V. Varadan, and V. K. Varadan, "Scattering of acoustic waves by layered elastic and viscoelastic obstacles in water," *J. Acoust. Soc. Am.* **68**, 673-685 (1980).
19. B. Peterson and S. Strom, "Matrix formulation of acoustic scattering from an arbitrary number of scatterers," *J. Acoust. Soc. Am.* **56**, 771-780 (1974).

20. V. K. Varadan, V. V. Varadan, and Y. Pao, "Multiple scattering of elastic waves by cylinders of arbitrary cross section. I. SH waves," *J. Acoust. Soc. Am.* **63**, 1310-1319 (1978).
21. A. Bostrom, "Multiple scattering of elastic waves by bounded obstacles," *J. Acoust. Soc. Am.* **67**, 399-413 (1980).
22. V. V. Varadan and V. K. Varadan, "Configurations with finite numbers of scatterers--A self-consistent T-matrix approach," *J. Acoust. Soc. Am.* **70**, 213-217 (1981).
23. R. Lim and R. H. Hackman, "A formulation of multiple scattering by many bounded obstacles using a multicentered T supermatrix," *J. Acoust. Soc. Am.* **91**, 613-638 (1992).
24. B. Peterson and S. Strom, "Matrix formulation of acoustic scattering from multilayered scatterers," *J. Acoust. Soc. Am.* **57**, 2-13 (1975).
25. A. Bostrom, "Scattering of acoustic waves by a layered elastic obstacle in a fluid--An improved null field approach," *J. Acoust. Soc. Am.* **76**, 588-593 (1984).
26. Y. Yeh and Y. Pao, "On the transition matrix for acoustic waves scattered by a multilayered inclusion," *J. Acoust. Soc. Am.* **81**, 1683-1687 (1987).
27. V. V. Varadan, "Scattering matrix for elastic waves. II. Application to elliptic cylinders," *J. Acoust. Soc. Am.* **63**, 1014-1024 (1978).
28. V. K. Varadan, V. V. Varadan, L. R. Dragonette, and L. Flax, "Computation of rigid body scattering by prolate spheroids using the T-matrix approach," *J. Acoust. Soc. Am.* **71**, 22-25 (1982).
29. R. H. Hackman, "The transition matrix for acoustic and elastic wave scattering in prolate spheroidal coordinates," *J. Acoust. Soc. Am.* **75**, 35-45 (1984).
30. A. Lakhtakia, V. K. Varadan, and V. V. Varadan, "Iterative extended boundary condition method for scattering by objects of high aspect ratios," *J. Acoust. Soc. Am.* **76**, 906-912 (1984).
31. R. H. Hackman and D. G. Todoroff, "An application of the spheroidal-coordinate-based transition matrix: The acoustic scattering from high aspect ratio solids," *J. Acoust. Soc. Am.* **78**, 1058-1071 (1985).
32. A. Lakhtakia, V. V. Varadan, and V. K. Varadan, "Scattering of ultrasonic waves by oblate spheroidal voids of high aspect ratios," *J. Appl. Phys.* **58**, 4525-4530 (1985).
33. G. Kristensson and S. Strom, "Scattering from buried inhomogeneities--a general three-dimensional formalism," *J. Acoust. Soc. Am.* **64**, 917-936 (1978).
34. R. Lim, "Multiple scattering by many bounded obstacles in a multilayered acoustic medium," *J. Acoust. Soc. Am.* **92**, 1593-1612 (1992).
35. R. H. Hackman and G. S. Sammelmann, "Acoustic scattering in an inhomogeneous waveguide: Theory," *J. Acoust. Soc. Am.* **80**, 1447-1458 (1986).
36. G. S. Sammelmann and R. H. Hackman, "Acoustic scattering in a homogeneous waveguide," *J. Acoust. Soc. Am.* **82**, 324-336 (1987).
37. R. H. Hackman and G. S. Sammelmann, "Multiple-scattering analysis for a target in an oceanic waveguide," *J. Acoust. Soc. Am.* **84**, 1813-1825 (1988).



38. J. D. Jackson, *Classical Electrodynamics*, Second Edition (John Wiley & Sons, Inc., New York, 1975) page 742.
39. S. Strom, "T matrix for electromagnetic scattering from an arbitrary number of scatterers with continuously varying electromagnetic properties," *Phys. Rev. D* **10**, 2685-2690 (1974).
40. P. M. Morse and H. Feshbach, *Methods of Mathematical Physics, Parts I and II* (McGraw-Hill, New York, 1953).
41. V. D. Kupradze, "Dynamical Problems in Elasticity," in *Progress in Solid Mechanics*, edited by I. N. Snedden and R. Hill (North-Holland, Amsterdam, 1963), Vol. 3.
42. P. G. Richards, "Weakly coupled potentials for high-frequency elastic waves in continuously stratified media," *Bull. Seismol. Soc. Am.* **64**, 1575-1588 (1979).
43. K. E. Hawker, S. R. Rutherford, and P. J. Vidmar, "A Summary of the Results of a Study of Acoustic Interaction with the Sea Floor," Applied Research Laboratories Technical Report No. ARL-TR-79-2, Applied Research Laboratories, The University of Texas at Austin, Austin, Texas (1979).
44. P. J. Vidmar, "The effect of sediment rigidity on bottom reflection loss in a typical deep sea sediment," *J. Acoust. Soc. Am.* **68**, 634-638 (1980).
45. G. J. Fryer, "Compressional-shear wave coupling induced by velocity gradients in marine sediments," *J. Acoust. Soc. Am.* **69**, 647-660 (1981).
46. M. V. Hall, "Acoustic reflectivity of a sandy seabed: A semianalytic model of the effect of coupling due to the shear modulus profile," *J. Acoust. Soc. Am.* **98**, 1075-1089 (1995).
47. T. Yamamoto, "Velocity variabilities and other physical properties of marine sediments measured by crosswell acoustic tomography," *J. Acoust. Soc. Am.* **98**, 2235-2248 (1995).
48. P. G. Richards, "Potentials for elastic displacement in spherically symmetric media," *J. Acoust. Soc. Am.* **50**, 188-197 (1971).
49. W. M. Ewing, W. S. Jardetsky, F. Press, *Elastic Waves in Layered Media*, (McGraw-Hill, New York, 1957) page 329.
50. R. N. Gupta, "Reflection of Elastic Waves from a Linear Transition Layer," *Bull. Seismol. Soc. Am.* **56**, 511-526 (1966).
51. E. L. Hamilton, "Geoacoustic modeling of the sea floor," *J. Acoust. Soc. Am.* **68**, 1313-1340 (1980).